Received: 15 September 2020 | Accepted: 9 October 2020 | Published online: 5 February 2021

DOI: 10.1002/trc2.12106

Alzheimer's & Dementia
Translational Research & Clinical Interventions

RESEARCH ARTICLE

Rasagiline effects on glucose metabolism, cognition, and tau in Alzheimer's dementia

Dawn C. Matthews[1] | **Aaron Ritter**[2] | **Ronald G. Thomas**[3] | **Randolph D. Andrews**[1] | **Ana S. Lukic**[1] | **Carolyn Revta**[4] | **Jefferson W. Kinney**[5] | **Babak Tousi**[6] | **James B. Leverenz**[7] | **Howard Fillit**[8] | **Kate Zhong**[9] | **Howard H. Feldman**[10] | **Jeffrey Cummings**[2,11]

[1] ADM Diagnostics, Inc., Northbrook, Illinois, USA

[2] Cleveland Clinic Lou Ruvo Center for Brain Health, Las Vegas, Nevada, USA

[3] Department of Family Medicine and Public Health, UCSD, La Jolla, California, USA

[4] Alzheimer's Disease Cooperative Study, University of California San Diego School of Medicine, La Jolla, California, USA

[5] Department of Brain Health, University of Nevada Las Vegas, Las Vegas, Nevada, USA

[6] Neurologic Institute, Cleveland Clinic, Cleveland, Ohio, USA

[7] Cleveland Clinic Lou Ruvo Center for Brain Health, Cleveland, Ohio, USA

[8] Alzheimer's Drug Discovery Foundation, New York, New York, USA

[9] CNS Innovations, LLC, Henderson, Nevada, USA

[10] Department of Neurosciences, Alzheimer's Disease Cooperative Study, San Diego, University of California, La Jolla, California, USA

[11] Department of Brain Health, Chambers-Grundy Center for Transformative Neuroscience, School of Integrated Health Sciences, University of Nevada Las Vegas, Nevada, USA

Correspondence
Dawn C Matthews, ADM Diagnostics, Inc., 555 Skokie Blvd., Suite 500, Northbrook, IL 60062.
Email: dmatthews@admdx.com

Funding information This study was funded by the Alzheimer's Drug Discovery Foundation (ADDF). The ADDF did not influence the study protocol, data analysis, interpretation of results, or preparation of the article.

Abstract

Background: A Phase II proof of concept (POC) randomized clinical trial was conducted to evaluate the effects of rasagiline, a monoamine oxidase B (MAO-B) inhibitor approved for Parkinson disease, in mild to moderate Alzheimer's disease (AD). The primary objective was to determine if 1 mg of rasagiline daily for 24 weeks is associated with improved regional brain metabolism (fluorodeoxyglucose–positron emission tomography [FDG-PET]) compared to placebo. Secondary objectives included measurement of effects on tau PET and evaluation of directional consistency of clinical end points.

Methods: This was a double-blind, parallel group, placebo-controlled, community-based, three-site trial of 50 participants randomized 1:1 to receive oral rasagiline or placebo (NCT02359552). FDG-PET was analyzed for the presence of an AD-like pattern as an inclusion criterion and as a longitudinal outcome using prespecified regions of interest and voxel-based analyses. Tau PET was evaluated at baseline and longitudinally. Clinical outcomes were analyzed using an intention-to-treat (ITT) model.

Results: Fifty patients were randomized and 43 completed treatment. The study met its primary end point, demonstrating favorable change in FDG-PET differences in rasagiline versus placebo in middle frontal ($P < 0.025$), anterior cingulate ($P < 0.041$), and striatal ($P < 0.023$) regions. Clinical measures showed benefit in quality of life ($P < 0.04$). Digit Span, verbal fluency, and Neuropsychiatric Inventory (NPI) showed non-significant directional favoring of rasagiline; no effects were observed in Alzheimer's Disease Assessment Scale-Cognitive Subscale (ADAS-cog) or activities of daily living. Rasagiline was generally well tolerated with low rates of adverse events and notably fewer neuropsychiatric symptoms in the active treatment group.

Discussion: These outcomes illustrate the potential benefits of rasagiline on clinical and neuroimaging measures in patients with mild to moderate AD. Rasagiline appears to affect neuronal activity in frontostriatal pathways, with associated clinical benefit potential warranting a more fully powered trial. This study illustrated the potential benefit of therapeutic repurposing and an experimental medicine proof-of-concept design with biomarkers to characterize patient and detect treatment response.

KEYWORDS
Alzheimer's disease, dopamine, FDG-PET, flortaucipir, glucose metabolism, MAO-B, QoL-AD, rasagiline, tau PET

1 | INTRODUCTION

The need for effective therapeutics for patients with mild to moderate Alzheimer's disease (AD) is urgent, given limitations of currently approved medications and a high rate of negative clinical trial outcomes.[1] We conducted a Phase II "proof of concept" (POC) randomized clinical trial to evaluate the potential benefit of rasagiline in patients with mild to moderate AD. Rasagiline is a selective monoamine oxidase B (MAO-B) inhibitor approved for treatment of Parkinson disease (PD) that has been shown to be safe and well-tolerated. MAO-B inhibition increases the availability of dopamine, which mediates cognitive functions including executive abilities, working memory, attention, and reward as well as motor function.[2] In nonclinical AD models, rasagiline has demonstrated potential neuroprotection, with reductions in amyloid accumulation, tau hyperphosphorylation, and neurofibrillary tangle formation.[3,4]

Studies of rasagiline in patients with PD and schizophrenia suggest that the agent produces cognitive and other clinical benefits.[5–7] Selegiline, a related MAO-B inhibitor, has shown cognitive benefit in AD and PD,[8–10] and phase II and III trials of the MAO-B inhibitor lazabemide in AD patients demonstrated benefit in several cognitive and behavioral endpoints.[11] However, some clinical studies of MAO-B inhibitors have shown mixed or negative results. For example, sembragiline did not meet cognitive or functional end points in AD patients over 52 weeks, but neuropsychiatric and functional benefit was noted in the more impaired subgroup. Ladostigil showed potential atrophy-slowing effects but did not significantly alter clinical progression in mild cognitive impairment patients.[12,13] No trial has examined the effects of rasagiline on functional brain networks and relationship to clinical benefit. The present study sought to understand the rasagiline as a potential treatment for patients with mild to moderate AD, supported by imaging of neuronal function and tau pathology.

The primary end point was change in cerebral glucose metabolism measured using fluoro-2-deoxyglucose (FDG) positron emission tomography (PET), demonstrated to correspond to disease progression and functional treatment effects.[14,15] Based on prior studies,[16] we hypothesized that FDG changes would be measurable with greater power over a shorter duration than clinical effects and could aid in understanding the biological basis for potential clinical outcomes. FDG-PET was also used to evaluate the presence of an AD-like pattern of glucose metabolism as an enrollment prerequisite, increasing confidence in a diagnosis of AD. A progressive pattern of temporoparietal hypometabolism has been reported to differentiate AD from other dementias, correlate with clinical status,[17] and to be consistent with brain amyloidopathy.[18] Clinical end points were evaluated as secondary outcomes to verify directional consistency with FDG.

This trial also included longitudinal measurement of tau with flortaucipir (Tauvid; Avid Radiopharmaceuticals) as a measure of AD pathology. Tau aggregation is observed early in AD in medial temporal regions, spreading to lateral temporal, posterior, and frontal neocortex as AD progresses.[19–21] Tau increases have been detected over periods as short as 9 months.[22] This trial expanded on prior studies by measuring tau changes over a shorter period of 24 weeks and a broad range of AD severity, concurrent with FDG-PET.

HIGHLIGHTS

- Rasagiline is a monoamine oxidase B inhibitor approved in Parkinson disease.
- Rasagiline was evaluated in patients with mild to moderate Alzheimer's disease.
- A beneficial effect on frontostriatal glucose metabolism was observed versus placebo.
- Directional changes in quality of life and cognition supported clinical benefit.
- Relationships were observed between tau, other biomarkers, and treatment effect.

RESEARCH IN CONTEXT

1. Systematic review: The authors reviewed the literature using PubMed, meeting abstracts and presentations, and other on-line searches. Relevant publications regarding studies of monoamine oxidase B (MAO-B) inhibitors and imaging biomarkers used in the study were cited.
2. Interpretation: This double-blind, placebo-controlled experimental medicine study of the effects of rasagiline in Alzheimer's disease (AD) met its primary outcome of improved or mitigated decline of glucose metabolism in the treatment group compared to placebo. Directional changes consistent with treatment benefit were observed in some measures of cognition, including those mediated by frontal subcortical systems sensitive to dopaminergic effects, and quality of life.
3. Future Directions: Improved treatments for patients with mild-to-moderate AD are needed. Repurposed agents offer a means of developing new therapies while shortening development times and reducing cost. This study suggests that rasagiline warrants further evaluation as a repurposed therapy for AD, and illustrates a proof-of-concept (POC) study design as a model for other studies.

2 | METHODS

2.1 | Study design

This was a double-blinded, randomized, placebo-controlled study of the effects of 0.5 mg of rasagiline daily followed by 5 months of 1 mg of oral rasagiline daily in 50 patients with mild to moderate AD (clinicaltrials.gov NCT02359552). The study was conducted after institutional review board approval with informed consent. Key inclusion criteria were a clinical diagnosis of probable AD (National Institute of Neurological and Communicative Disorders and Stroke and the Alzheimer's Disease and Related Disorders Association (NINDS-ADRDA) criteria), age 50 to 90 years, Mini-Mental State Exam (MMSE) 12-26, and Fluorodeoxyglucose Positron Emission Tomography (FDG-PET) pattern of hypometabolism consistent with AD.[23] Exclusion factors included neurologic, radiologic, or laboratory indications of non-AD dementia; medications that might interact with rasagiline; and factors that might lead to inability to complete the study. Patients on stable doses of cholinesterase inhibitors and memantine for at least 3 months prior to randomization were permitted. No dose changes were permitted during the study.

The primary outcome measure of this exploratory trial was the change from baseline to week 24 in FDG-PET in pre-specified AD-relevant regions including medial and lateral temporal, posterior cingulate-precuneus, inferior parietal, and middle frontal cortices. The anterior cingulate and striatum, relatively preserved in late AD, were prespecified given their glucose metabolic correlation with dopamine[24] and a reported increase in striatal glucose metabolism with associated neuropsychiatric benefit following selegiline administration.[25] A voxel-based data-driven pattern derived from a multivariate machine learning analysis of baseline and 24-week scans was evaluated. This approach measures multi-region response as a single end point, taking into account relationships between regions.

Secondary outcome measures included change in tau measured by flortaucipir PET over 24 weeks; safety and tolerability; and the following clinical end points: Alzheimer's Disease Assessment Scale–Cognitive Subscale (ADAS-cog), MMSE, Digit Span (DS), Controlled Oral Word Association Test (COWAT), Alzheimer's Disease Cooperative Study-Clinical Global Impression of Change (ADCS-CGIC), ADCS Activities of Daily Living (ADL) scale, Quality of Life-AD (QoL-AD, with study partner), and Neuropsychiatric Inventory (NPI).

2.2 | Randomization

The study was conducted by the Cleveland Clinic Lou Ruvo Center for Brain Health at three sites (Las Vegas NV, Cleveland OH, Lakewood OH). Randomization was stratified by site, performed by the research pharmacist using a predetermined randomization schedule in which participants were assigned to rasagiline or placebo in a 1:1 ratio using randomly generated blocks of four or six participants.

2.3 | Statistical power

Prior FDG-PET studies showed that metabolic changes associated with cognitive effects in AD can be detected in an unpaired design with less than 20 participants per arm.[14] Disease-related decline can be detected, although powered measurement of mitigation requires additional participants or time.[16] The study was not powered for clinical significance, but—as an experimental medicine approach—was designed to assess directionality for consistency with FDG findings and to determine the number of participants required to show a rasagiline-placebo difference in a powered trial.

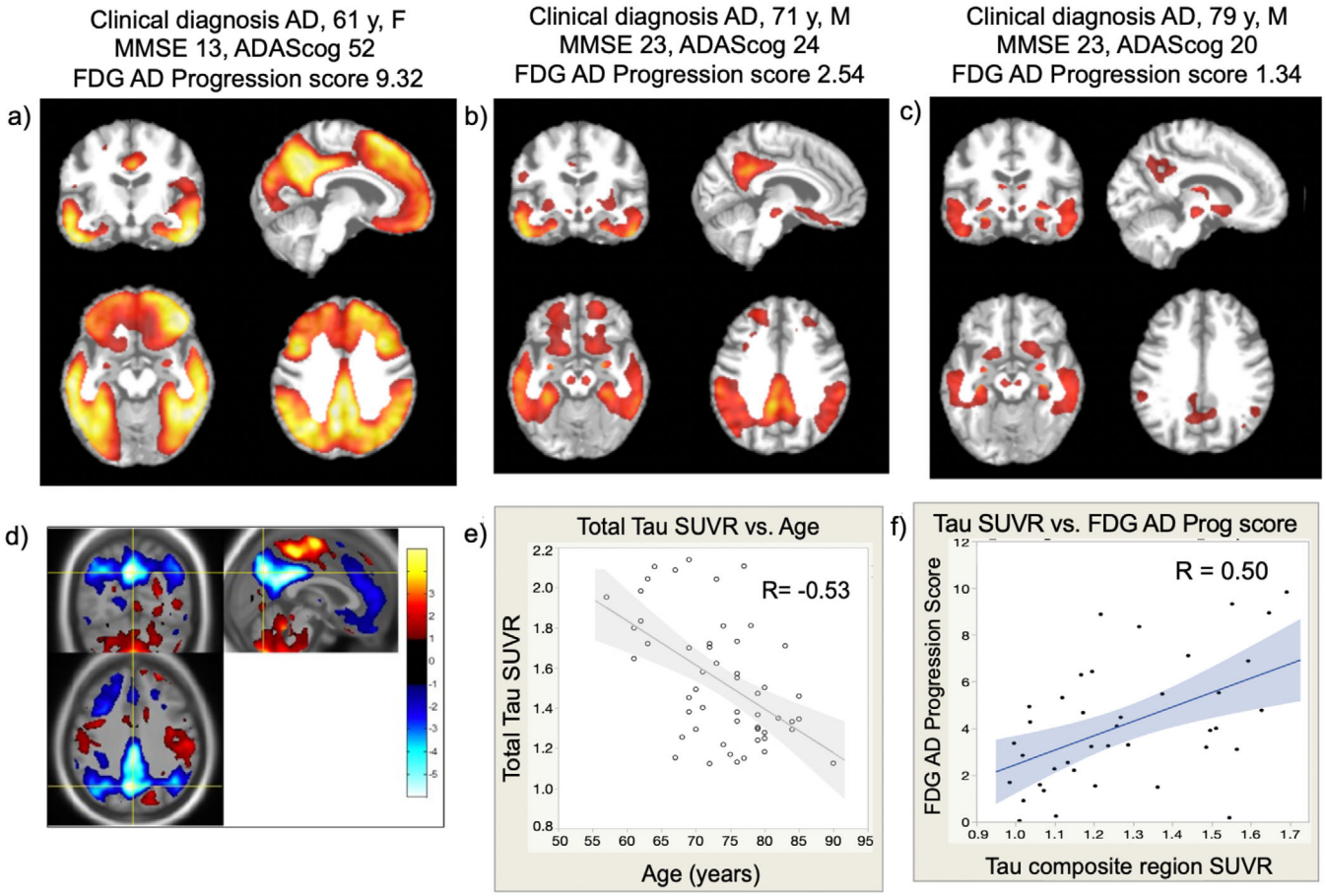

FIGURE 1 **Baseline FDG and Tau burden**. a-c, Tau burden for three participants age 61, 72, and 79 years shown with baseline clinical and FDG scores. d, Pattern of hypometabolism and preservation relative to whole brain that is quantified by the AD Progression score. e, Relationship between participant age and total tau SUVR. f, Relationship between tau burden in a composite of temporal and parietal regions involved in the pattern of (d) versus FDG-AD Progression score

2.4 | Procedures

2.4.1 | Medication

Rasagiline was initiated at 0.5 mg once daily for 4 weeks, increased to a 1 mg dose once daily at week 5, and maintained at this dose until the end of week 24. Active and placebo tablets were provided by Teva, re-coated identically, and repackaged by randomization ID in a blinded manner.

2.4.2 | Image acquisition and measurement

MRI was acquired at screening, and FDG and flortaucipir PET imaging were performed at baseline and at week 24. Images were acquired using protocols based upon the Alzheimer's Disease Neuroimaging Initiative (ADNI, www.adni-info.org) and processed as described in the Supplemental Material.

Each participant's baseline FDG-PET scan was evaluated using two previously developed image classifiers that use a single time point. The first was trained to differentiate scans of persons having status of amyloid negative and cognitively normal, amyloid positive with various stages of MCI and AD, frontotemporal dementia, and dementia with Lewy bodies (DLB). The second quantifies the degree to which a scan expresses a pattern of hypometabolism and preservation relative to whole brain that reflects the progression of AD from amyloid negative, cognitively normal status through amyloid-positive AD dementia. This pattern (Figure 1d) is characterized by hypometabolism in posterior cingulate, precuneus, inferior parietal, and temporal cortices, and correlates with subsequent rate of cognitive decline.[23] Participants were included if their highest probability class was on the AD spectrum, with or without indication of secondary disease such as DLB.

FDG Standardized Uptake Value ratios (SUVRs) were measured and compared using different reference regions to confirm that changes were not driven by a single reference. Data-driven multivariate machine learning was applied to identify voxel intensity patterns characterizing differences between treatment arms. Scans were grouped into classes based upon visit (baseline, 24 weeks), study arm, and age (younger, older), and input to the classifier software. The software used Principal Component Analysis (PCA), Canonical Variate Analysis (mathematical combinations of PCs), and intensive iterative split-half data resampling to determine the pattern(s) that best discrim-

inated groups while minimizing data overfitting.[26] Pattern expression was quantified as a numeric score for each participant.

Tau SUVRs were measured in cortical tissue excluding cerebellum; a composite temporal region, the regions measured for FDG-PET; and using an adaptive approach that measured the change in subject-specific set of voxels that were suprathreshold at baseline or 24 weeks to avoid directional bias, standardized to a common total volume. White matter and cerebellar cortex reference regions were defined using a Gaussian decomposition approach (PERSI) (Supplement).[27]

2.4.3 | Clinical end points

The ADAS-cog, NPI, ADCS-ADL, DS, and COWAT were administered at baseline, and at weeks 4, 8, 24, and 28. MMSE was administered at screening, baseline, and 24 weeks. The CGIC was collected at 4, 8, 24, and 28 weeks. QoL-AD was administered at baseline and 24 weeks. Safety was monitored through weekly review of adverse events throughout the study.

2.4.4 | Statistical analysis

Participants who completed both PET visits and passed image quality control were evaluated longitudinally. Six-month changes in SUVR values and classifier scores were compared between treatment arms by ANOVA adjusted for age, baseline values, and interaction terms when applicable (JMP v14 (SAS); G:Power software). Comparisons were also made within younger and older age strata given reports of greater tau and more rapid progression in younger AD participants[20] and potential comorbidities that may influence outcomes in older participants. Statistical comparisons were based on absolute change values.

Mixed-model repeated-measures analyses were used to assess between-group clinical end point differences in modeled change over 24 weeks. The dependent variable was the change from baseline score. Fixed effects were baseline outcome measure scores, treatment arm, visit, and treatment-by-visit interaction. Study visit was treated as a continuous variable; an unstructured variance–covariance matrix was used. The primary efficacy analysis was based on the modified intention-to-treat (mITT) population, including all randomly assigned participants with at least one post-baseline observation. Testing for treatment differences was conducted by assessing the statistical significance of the treatment-by-visit regression coefficient. Relationships between clinical and imaging end points were explored using correlation (Pearson R). Because this was a preliminary POC study, no adjustments for multiple comparisons were made and a two-sided *P*-value of 0.05 was considered significant.

In addition to including baseline values as model covariates, methods were implemented to further assess the impact of baseline differences on outcomes. The software package "designmatch"[28] was used to match treatment and placebo groups for MMSE, ADL, ADAS, and QoL-AD at baseline. T-test and Analyses of Covariance (ANCOVAs) were run on the reduced set. A Cochran-Mantel-Haenszel test was performed on the full data set, splitting the sample at the median for the MMSE (score of 20). Pre-defined exploratory analyses evaluated treatment effects for all clinical end points by baseline clinical severity measured by MMSE.

3 | RESULTS

3.1 | Participants

Between May 19, 2015 and January 26, 2018, 96 participants were screened, of whom 50 were randomized to rasagiline or placebo and 43 completed treatment. Of the 25 placebo participants, 3 were lost to follow-up (delusions, stroke, worsening pseudobulbar/other effects), and one did not have a week-24 FDG PET scan, resulting in 21 placebo participants for image analysis. Of the 25 participants in the rasagiline arm, 4 were lost to follow-up (broken hip/rib, atrial fibrillation, other non-adverse event factors) (Figure S1).

Table 1 shows the demographic and baseline clinical characteristics of enrolled patients by treatment arm. Age, sex, education, genotype, and baseline NPI, DSPAN, and COWAT scores did not differ between groups. MMSE and ADAS-cog baseline scores were more impaired (by chance) in the placebo arm than the rasagiline arm ($P < 0.06$), whereas the rasagiline arm had worse baseline QoL-AD scores ($P < 0.02$). Of the 43 participants who completed the study, one did not have a week-24 FDG PET scan and 3 were excluded from analysis due to pre-specified behavioral or motion confounds during image acquisition. Among the 39 participants included in longitudinal image analysis, baseline MMSE and ADAS-cog scores did not differ between groups and QoL-AD scores were worse in the rasagiline-treated group ($P < 0.05$).

3.2 | Baseline PET and ApoE characterization

Of the 59 participants whose screening FDG scans were analyzed using the Dementia Classifier, 57 exhibited a pattern of hypometabolism classified as AD-like and were included for potential enrollment. Seventy-one percent of participants were apolipoprotein E gene (*APOE*) $\varepsilon 4$ variant carriers, consistent with trials where positive amyloid imaging is used as an entry criterion.[29] Participants were diverse in FDG AD Progression Classifier scores (Figure 1f), which correlated with baseline MMSE ($R = -0.44$, $P < 0.001$) and ADAS-cog scores ($R = 0.42$, $P < 0.003$). AD Progression score and baseline MMSE did not differ significantly between study arms in the PET analysis population.

Tau burden varied widely across participants (Figures 1a-c) but did not differ between treatment arms. Tau was associated with age (Figure 1e), as younger participants (age 57 to 69 years) exhibited pervasive burden while oldest participants (late 70s to 90) had lower, primarily temporal burden with smaller posterior clusters, and patients in their 70s showed a wide range. Spatial patterns varied in asymmetry and occipital involvement. Forty-seven of the 50 participants (94%) had readily visualized elevated flortaucipir and positive regional SUVRs,

TABLE 1 Baseline demographic and clinical characteristics of the study population

Mean (std dev)	Placebo (N = 25)	Rasagiline (N = 25)	All (N = 50)	*P*-value (Placebo vs Rasagiline)
Age (range)	73.4 (7.1) (57 - 84)	74.7 (7.4) (62 - 90)	74 (7.2) (57 - 90)	0.53
Gender (F/M)%	44 / 56	56 / 44	50 / 50	0.60
Education	14 (2)	14 (3	14 (3)	0.83
ADAS-Cog	28 (11)	23 (6)	26 (9)	**0.06**
MMSE	19 (5)	21 (4)	20 (4)	**0.06**
ADL	58 (11)	62 (8)	60 (10)	0.20
NPI	8 (9)	8 (8)	8 (8)	0.78
DSPAN	12 (3)	13 (3)	12 (3)	0.13
COWAT	21 (13)	27 (13)	24 (13)	0.13
QOL-AD	40 (5)	36 (6)	38 (6)	**0.02**
APOE 2/3	4%	4%	4%	0.50
2/4	0%	4%	2%	
3/3	16%	29%	22%	
3/4	60%	38%	49%	
4/4	20%	25%	22%	
AChEI(s)	84%	84%	84%	1.00
Memantine	44%	40%	42%	0.78
Antidepressant(s)	36%	56%	46%	0.16
Anxiolytic(s)	4%	4%	4%	1.00
Antipsychotic(s)	8%	4%	6%	0.56
site id 1	48%	52%	50%	1.00
site id 2	36%	36%	36%	
site id 3	16%	12%	14%	

while three had threshold cortical SUVR values (1.3). Total tau correlated with FDG AD Progression classifier score ($R = -0.41$, $P < 0.003$).

3.3 | Trial outcomes

3.3.1 | Primary end point

The study met its primary end point of improvement in longitudinal glucose metabolism in rasagiline-treated participants versus placebo in one or more prespecified regions and in the pattern determined through voxel-based analysis (Figure 2a,b). Rasagiline-treated participants decreased less than placebo-treated participants in middle frontal cortex (left $P < 0.012$, E.S. 0.82; bilateral $P < 0.025$, E.S. 0.75), anterior cingulate cortex ($P < 0.043$, E.S. 0.68), striatum ($P < 0.02$, E.S. 0.83) (Table 2) and in the voxel-based classifier-derived pattern ($P < 0.02$, Figure 2b), which was consistent with regional effects. Treatment effects remained significant when including age, baseline SUVR, and baseline MMSE as covariates. Age was a significant covariate for middle frontal cortex and striatum. Results using whole brain, subcortical white matter, and pons as alternate reference regions were in agreement regarding affected regions and directionality.

Placebo arm FDG AD Progression scores increased in severity ($P < 0.01$), and regional SUVRs likewise decreased in posterior cingulate-precuneus ($P < 0.03$, E.S. 0.74), inferior parietal ($P < 0.01$, E.S. 0.86), and middle frontal ($P < 0.001$, E.S. 1.74) regions, with decline greater in younger participants.

3.3.2 | Secondary end points

Longitudinal clinical end points for the rasagiline and placebo arms over 24 weeks are presented in Figure 3. A favorable outcome for rasagiline compared to placebo was observed for QoL-AD ($P < 0.04$ all participants, adjusted for baseline QoL; $P < 0.07$ with a reduced set of matched baseline participants and adjusted for baseline QoL and MMSE; $P < 0.07$ Mantel-Haenszel chi-square). In particular, uniform improvements were observed in rasagiline-treated participants compared to decline in placebo participants with similar baseline values (Figure 3b,c), and trajectories were clearly separated in the matched baseline analysis of all ages (Figure 3d). Directionally favorable outcomes were observed in Digit Span, CGIC, COWAT, and NPI. No significant differences were observed in ADL and ADAS-cog (Figure 3a, Table S1). Mean values for each time point and results for pre-specified

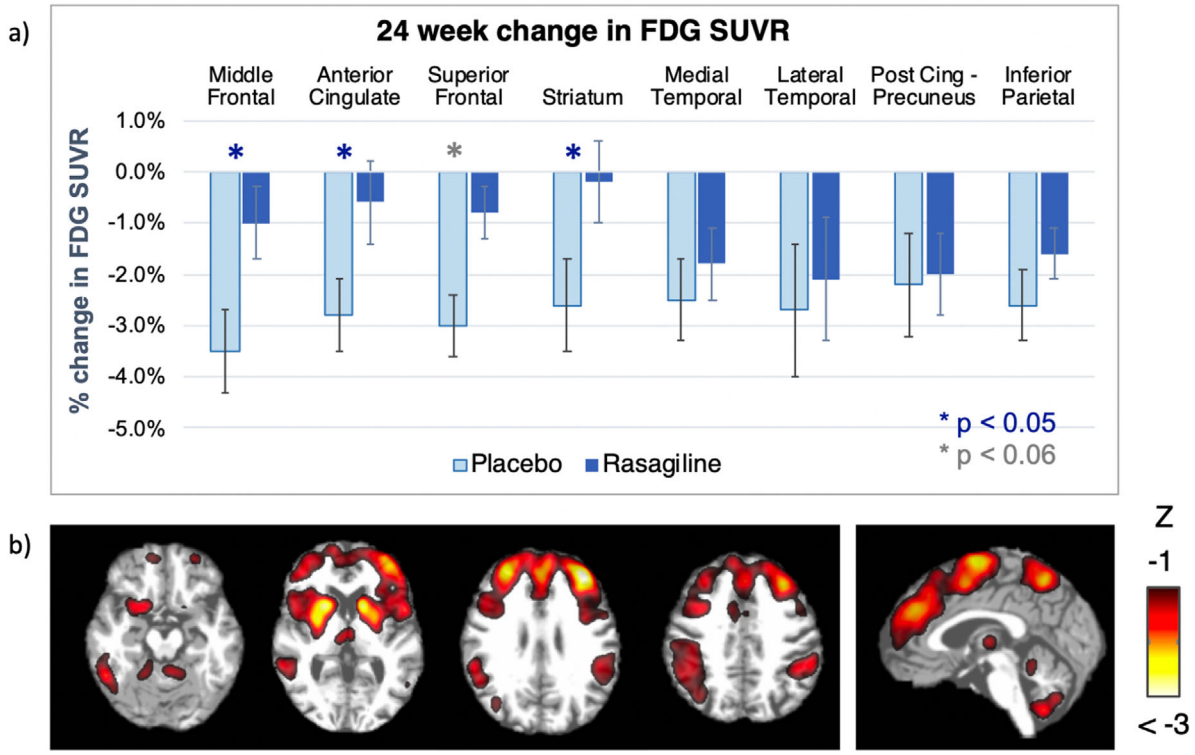

FIGURE 2 a, Twenty-four-week change in FDG SUVR in placebo- versus rasagiline-treated patients. b, Longitudinal voxel-based classifier results showing regions where rasagiline-treated participants declined less in glucose metabolism than placebo-treated participants

MMSE strata are shown in the Supplementary Material. There were no side effects.

Increases in tau PET were observed in some participants over 24 weeks, particularly those with higher baseline values (Figure 4a,b). Greater slopes and statistical power were observed when using the adaptive method that defined the region of interest according to combined pre- or post-suprathreshold voxels (Figure 4b). No treatment differences in change in flortaucipir were observed in cortical regions having suprathreshold values at baseline. Uniform longitudinal decreases were observed in the rasagiline but not placebo arm in subcortical regions, particularly accumbens ($P < 0.0001$) and putamen ($P < 0.003$) (Supplement).

3.3.3 | Relationships between imaging and clinical end points

Higher tau burden, lower glucose metabolism, and lower cortical thickness in temporal regions at baseline correlated with greater decline in MMSE score in placebo participants ($P < 0.008$, $P < 0.05$, $P < 0.004$, respectively). These relationships (Figure S2a) were not seen in rasagiline trajectories, which were relatively stable or improved independent of these baseline values. Longitudinal differences between rasagiline and placebo arms were most pronounced in participants having greater tau, lower metabolism, and lower volumes in temporal regions at baseline. Change in QoL-AD score, which differed between placebo and rasagiline arms, correlated with a pattern of increased metabolism in anterior cingulate, frontal, and striatal regions (Figure S2b,c) and with FDG SUVR increases in these regions (anterior cingulate R = 0.47, $P < 0.002$, caudate R = 0.47, $P < 0.002$) (Figure S2d).

3.3.4 | Safety and tolerability

Rasagiline was generally well tolerated, with neuropsychiatric adverse events (AEs) in 5 (20%) placebo and 0 (0%) rasagiline patients, non-neuropsychiatric AEs in 10 (40%) placebo and 13 (52%) rasagiline patients, and no treatment-related deaths (Table S2). No rasagiline-treated participants experienced neuropsychiatric symptoms of agitation/irritability or psychosis compared to five placebo participants (*t* test not significant).

4 | DISCUSSION

4.1 | Rasagiline effects

This investigation of rasagiline as a treatment for AD met its primary outcome of demonstrating improvements or less decline in glucose metabolism changes in prespecified regions compared to placebo over 24 weeks. FDG-PET findings suggested that rasagiline supports metabolic function in frontostriatal networks. Rasagiline prolongs dopamine availability through MAO-B inhibition, and results were consistent with previous studies that have established dopaminergic

TABLE 2 Region of interest results: difference (24 weeks minus baseline) mean, S.D. and difference between arms with 95% confidence interval

	Middle frontal	Anterior cingulate	Superior frontal	Striatum	Medial temporal	Lateral temporal	Post cing - precuneus	Inferior parietal
SUVRs								
Placebo	−0.032 (0.030)	−0.020 (0.021)	−0.016 (0.022)	−0.024 (0.029)	−0.015 (0.034)	−0.020 (0.029)	−0.017 (0.023)	−0.025 (0.029)
Rasagiline	−0.011 (0.030)	−0.003 (0.026)	−0.003 (0.018)	−0.002 (0.028)	−0.010 (0.034)	−0.016 (0.024)	−0.016 (0.018)	−0.018 (0.022)
Difference (95% CI)	0.020 (0.00–0.04)	0.016 (−0.00–0.03)	0.013 (0.00–0.04)	0.022 (0.00–0.04)	0.005 (−0.02–0.03)	0.005 (−0.01–0.02)	−0.001 (−0.01–0.01)	0.007 (−0.01–0.02)
Percentages								
Placebo	−3.5%	−2.8%	−2.0%	−2.6%	−2.5%	−2.7%	−2.2%	−2.6%
	(3.5%)	(3.1%)	(2.7%)	(3.1%)	(5.7%)	(4.4%)	(3.1%)	(3.5%)
Rasagiline	−1.0%	−0.6%	−0.4%	−0.2%	−1.8%	−2.1%	−2.0%	−1.6%
	(3.5%)	(3.1%)	(2.1%)	(3.1%)	(5.7%)	(4.4%)	(3.1%)	(3.5%)
Difference (95% CI)	2.5% (0.3-4.7%)	2.2% (0.1-4.3%)	1.6% (0.0-3.2%)	2.4% (0.2-4.3%)	0.8% (−2.4-4.0%)	0.6% (−1.8–3.0%)	0.2% (−1.5–1.9%)	0.9% (−1.5–3.3%)
P-values[a]	0.025	0.041	0.054	0.023	n.s.	n.s.	n.s.	n.s.

[a]based on the SUVR values and comparison of differences from baseline. Abbreviation: ns, not significant.

effects on frontostriatal neuronal function, with benefits on working memory and other cognitive function.[30,31] Because84% of participants in each arm of the present study were taking acetylcholinesterase inhibitors and/or medications such as memantine, rasagiline effects were incremental to the action of these medications.

The favorable effect in QoL observed for rasagiline was consistent with benefits on QoL reported with rasagiline in PD patients.[5,6] QoL has been associated in other studies with dopaminergic function.[31] Changes in DS, CGIC, COWAT, and NPI were directionally consistent with FDG results. The lack of ADAS-cog effect was similar to some studies of MAO-B inhibitors and rotigotine,[32] illustrating that a POC approach may efficiently identify end points for larger trials relevant to the cognitive signature of the treatment. The lower number of rasagiline-treated participants who spontaneously reported neuropsychiatric events compared to the placebo group suggests an additional effect worthy of further study. This observation supports the finding of a potential MAO-B inhibition effect on neuropsychiatric symptoms in AD patients reported in a phase 2 trial of sembragiline.[12]

Our findings indicate that differences associated with rasagiline treatment may be most detectable in participants exceeding baseline thresholds of temporal tau burden, hypometabolism, and atrophy (Figure S2). Prospective biomarker stratification may help focus analyses on subgroups in which benefit is greatest.

The longitudinal progression in AD classifier pattern in placebo group and the 2% to 3% differences between study arms in frontostriatal regions were similar to the magnitude of change observed in other FDG-PET studies of AD and central nervous system drugs.[14,15] The placebo group decreases in striatum, which is relatively preserved in late-onset AD, was driven by decreases in left caudate in younger patients. Caudate glucose metabolism has been identified as significantly reduced in early onset versus Late-onset AD.[33]

4.2 | Tau

This study illustrated the diverse distribution of tau in AD as well as its relationships to age, FDG-PET, and clinical status. Results suggest that tau accumulation is observable over periods as short as 24 weeks, with higher accumulation rates associated with higher baseline tau burden. Adaptive region definition increased change detection likely because it captured the diverse spatial distribution of tau across participants without diluting to entire cortex, and may minimize impact of head motion–induced tissue shifts by "ORing" pre- and post-suprathreshold boundaries.

Because rasagiline is a highly selective MAO-B inhibitor, this study provided a stringent test of possible MAO-B binding of flortaucipir. The uniform flortaucipir signal reductions observed in subcortical regions in rasagiline-treated but not placebo-treated participants may suggest binding to MAO-B. However, effects were very weak compared to MAO-B-binding reductions caused by a rasagiline dose equal to that in the present study[34] and to the signal depletion of [18F]THK5351, a tracer with strong MAO-B affinity, following rasagiline treatment[35] (further discussion in Supplement).

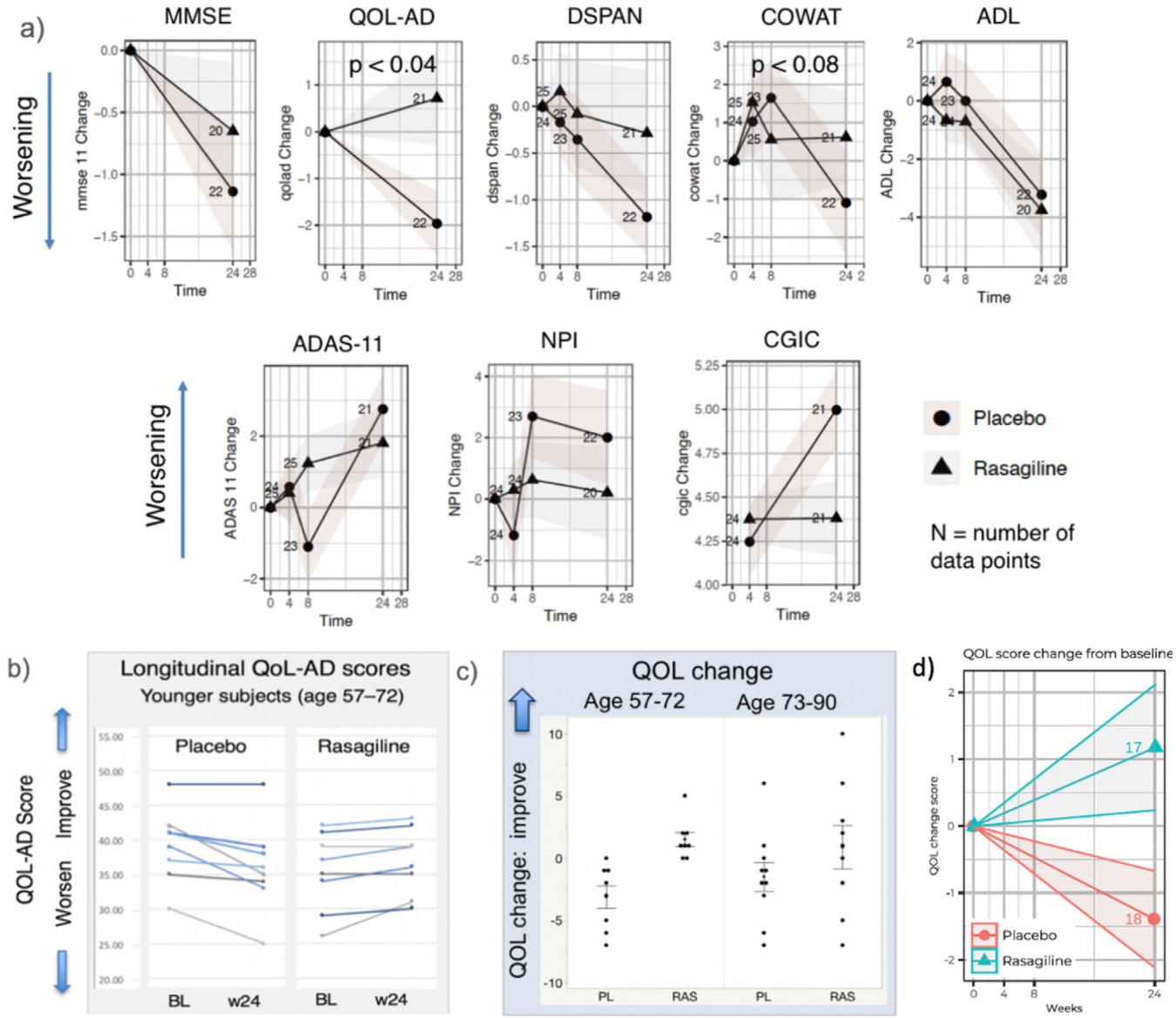

FIGURE 3 a, Longitudinal change in clinical end points by study arm. b, Individual participant longitudinal QoL-AD scores in the Younger subgroup. c, Change in QoL by study arm, younger, and older subgroups (PL = placebo, RAS = rasagiline treated). d, Change in QoL-AD from baseline in placebo and rasagiline group after matching for baseline clinical characteristics; decreases reflect worsening and increases represent improvement

4.3 | Study limitations

Limitations of the study include its small sample size and 24-week duration, intended for POC. The lack of amyloid measurement was a diagnostic limitation. However, flortaucipir, selective for AD variant tau, provided evidence of AD pathology and may serve as a surrogate indicator of amyloid given the observed relationship between neocortical tau and positive amyloid burden.[36,37] The high number of *APOE* ε4 carriers (71%) in the study is consistent with a trial population comprised primarily of AD patients.

The by-chance imbalance in baseline MMSE, ADAS-cog, and QoL scores between treatment arms posed a challenge also seen in other studies.[38,39] The multiple approaches applied to adjust for and/or balance these variables all supported the baseline-adjusted model results. However, imbalances impact analysis complexity and interpretation, and prospective approaches to balancing arms could aid in other trials.

4.4 | Conclusion

The findings of a favorable effect of rasagiline on longitudinal FDG over 24 weeks of treatment and directional benefit on clinical outcomes support a potential benefit of rasagiline for AD patients. Given that this is an available, generic treatment with substantial safety data, it would be a cost- and time-effective addition to available treatments. A

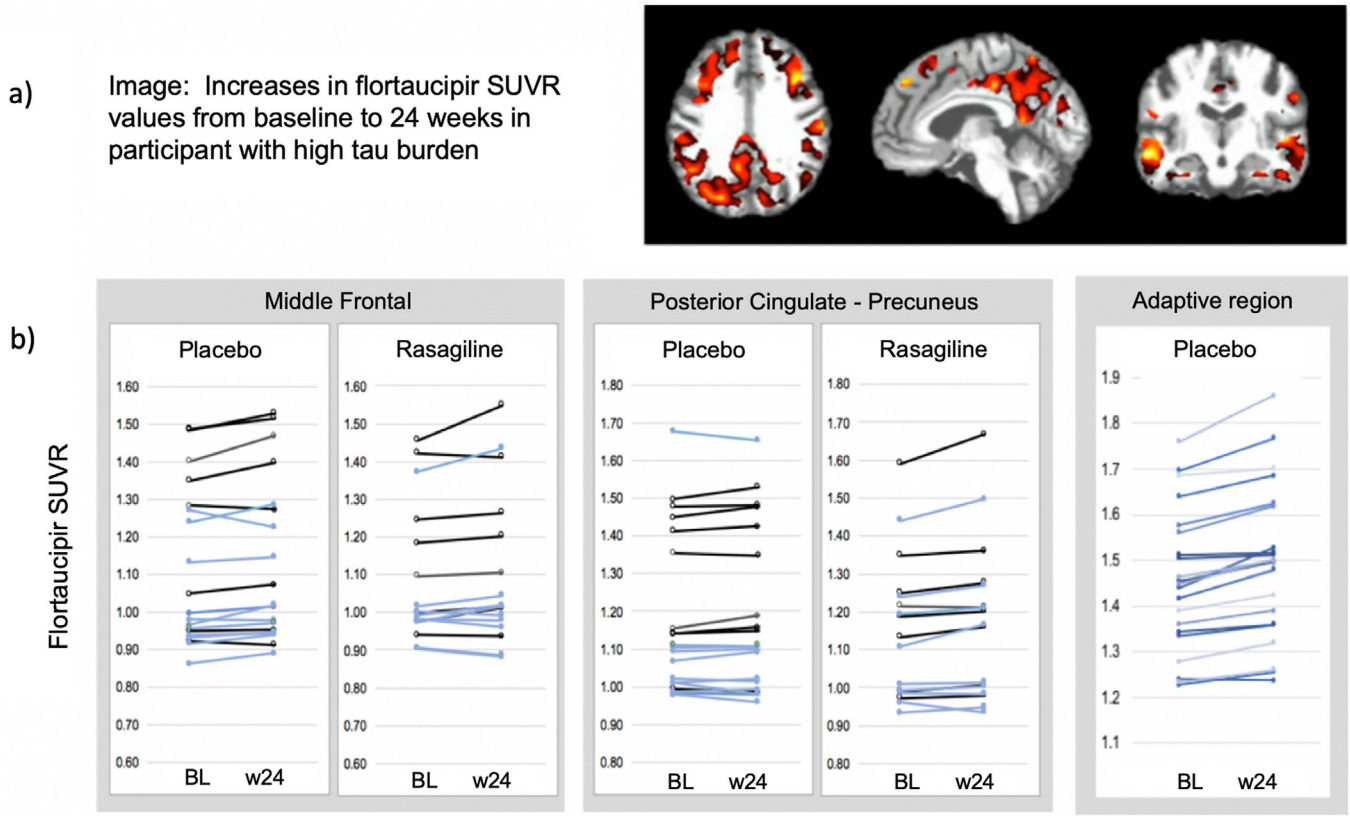

FIGURE 4 a, Example of increases in tau burden in a high tau imaging participant over 24 weeks. b, Twenty-four-week changes in flortaucipir SUVRs for middle frontal, posterior cingulate-precuneus, and an adaptive region determined by baseline and week 24 suprathreshold voxels, by study arm

powered clinical trial with assessment of QoL-AD, executive function, and neuropsychiatric aspects is warranted. More broadly, this study demonstrated the utility of a POC/experimental medicine design incorporating imaging biomarkers for participant inclusion, evaluation, and stratification as a path to increase the probability of success of larger AD trials.

ACKNOWLEDGMENTS

We would like to express our gratitude to the patients, families, and caregivers who participated in the study, and whose involvement made these findings and learning possible. We are grateful to Avid Radiopharmaceuticals (Eli Lilly) for providing the flortaucipir PET tracer for the study, to Teva Pharmaceuticals for providing rasagiline for the study, and to the Alzheimer's Drug Discovery Foundation (ADDF) for providing the funding for the study. We thank the following Cleveland Clinic members for their significant contributions to the clinical conduct of the study: Yolande Mucharbach, Christine Whitman, Hilda Sosic, Elaine Pienschke, Tami Kaczur, Sagar Patel, Nelson Rubina, and others who provided assistance. We thank Jennifer Mason and other members of the Alzheimer's Disease Coordinating Study (ADCS) for their roles in study database coordination and support; Michael Pontecorvo, Amanda Potasnik, Elisabeth DiPardo, and other members of Avid Radiopharmaceuticals for their assistance with flortaucipir imaging; and Anna Lu and Laura Matthews for their assistance with article preparation.

CONFLICTS OF INTEREST

Dawn C. Matthews, Randolph D. Andrews, and Ana S. Lukic are employees of ADM Diagnostics, Inc., which provides clinical trial imaging services and image analysis products. Carolyn Revta has received grants from Toyama Pharmaceuticals, Biohaven Pharmaceuticals, and Vivoryon (Probiodrug) during the conduct of the study. Babak Tousi has received a grant from the Alzheimer's Drug Discovery Foundation during the study. James B. Leverenz has received research support from the Alzheimer's Association, Avid Radiopharmaceuticals, Department of Defense, GE Healthcare, Lewy Body Dementia Association, Michael J Fox Foundation, National Institutes of Health, and Sanofi/Genzyme. Howard Fillit is founding Executive Director and Chief Science Officer of the Alzheimer's Drug Discovery Foundation, which funded the rasagiline clinical trial, and has provided consulting to the following pharmaceutical companies: Axovant, vTv, Lundbeck, Otsuka, Lilly, Biogen (RTI), Roche, Genentech, Merck, Samus, Pfizer, and Alector. Howard H. Feldman reports a service agreement through UCSD with the Cleveland Clinic for data management and biostatistics during the conduct of this study; grants from Toyama Pharmaceuticals, Biohaven Pharmaceuticals, and Vivoryon (Probiodrug); service agreements through UCSD for consulting with Eisai Pharmaceuticals, Merck Pharmaceuticals, Tau RX, Samus Therapeutics, Arkuda Therapeutics, Samumed, and Axon Neurosciences Roche/Genentech Pharmaceuticals for DMC and DSMB activities; Tau Consortium for Scientific Advisory Board; and Novo Nordisk for Advisory Board.

Jeffrey Cummings reports grants from National Institute of General Medical Sciences (NIGMS) COBRE grant #P20GM109025, during the conduct of the study; personal fees from Acadia, Actinogen, AgenBio, Alkahest, Alzheon, Avanir, Axsome, Biogen, Cassava, Cerecin, Cerevel, Cognoptix, Cortexyme, EIP, Eisai, Foresight, Green Valley, Grifols, Idorsia, Karuna, Nutricia, Orion, Otsuka, Probiodrug, QR Pharma, ReMYND, Resverlogix, Roche, Samumed, Samus Therapeutics, Third Rock, Signant Health, Sunovion, Suven, and United Neuroscience pharmaceutical and assessment companies; other from Alzheimer Drug Discovery Foundation; other from ADAMAS, BioAsis, MedAvante, QR Pharma, and United Neuroscience; personal fees from Neuropsychiatric Inventory (NPI), outside the submitted work; and is Chief Scientific Advisor for CNS Innovations. Aaron Ritter, Jefferson Kinney, Ronald G. Thomas, and Kate Zhong have nothing to disclose.

AUTHOR CONTRIBUTIONS

Jeffrey Cummings was the principal investigator of the trial, led the protocol design, and participated in article writing and editing. Dawn C. Matthews was the imaging lead for the study and the principal author of the article. Aaron Ritter was a lead clinical investigator for the trial and provided review and input to the protocol design and the article. Ronald G. Thomas provided the clinical end point statistical analysis and review of the article. Randolph D. Andrews and Ana S. Lukic provided image data quality control, processing, and analysis. Carolyn Revta contributed to data management, team coordination, and manuscript review. Jefferson W. Kinney provided *APOE* genotyping for the study. Babak Tousi and James B. Leverenz were clinical investigators for the trial and provided article review and input. Howard Fillit assisted in obtaining the flortaucipir PET tracer and study funding and provided article review. Kate Zhong provided input to study design, support in the conduct of the trial, and review and input for the article. Howard H. Feldman led the ADCS in providing clinical end point statistical analyses and overall study data management and provided editing and review of the article.

ETHICS APPROVAL AND CONSENT TO PARTICIPATE

The study was conducted under institutional review board approval with informed patient consent.

CONSENT FOR PUBLICATION

All appropriate author consents have been obtained. Other consent is not applicable.

AVAILABILITY OF DATA AND MATERIALS

Data have been published in clinicaltrials.gov and are being made available on-line by the Alzheimer's Disease Coordinating Study (ADCS).

REFERENCES

1. Cummings JL, Morstorf T, Zhong K. Alzheimer's disease drug-development pipeline: few candidates, frequent failures. *Alzheimers Res Ther*. 2014;6(4):37..
2. Nieoullon A. Dopamine and the regulation of cognition and attention. *Prog Neurobiol*. 2002;67(1):53-83.
3. Bar-Am O, Amit T, Weinreb O, Youdim MB, Mandel S. Propargylamine containing compounds as modulators of proteolytic cleavage of amyloid-beta protein precursor: involvement of MAPK and PKC activation. *J Alzheimers Dis*. 2010;21:361-371.
4. Jenner P, Langston JW, Explaining ADAGIO: A critical review of the biological basis for the clinical effects of rasagiline. *Mov Disord*. 2011;26(13):2316-2323. https://doi.org/10.1002/mds.23926. Epub 2011 Sep 23. PMID: 21953831
5. Krishna R, Ali M, Moustafa AA. Effects of combined MAO-B inhibitors and levodopa vs. monotherapy in Parkinson's disease. *Front Aging Neurosci*. 2014;6:180.
6. Biglan KM, Schwid S, Eberly S, et al. Rasagiline improves quality of life in patients with early Parkinson's disease. *Mov Disord*. 2006;21:616-623.
7. Hanagasi HA, Gurvit H, Unsalan P. The effects of rasagiline on cognitive deficits in Parkinson's disease patients without dementia: a randomized, double-blind, placebo-controlled, multicenter study. *Mov Disord*. 2011;26(10):1851-1858.
8. Dixit SN, Behari M, Ahuja GK. Effect of selegiline on cognitive functions in Parkinson's disease. *J Assoc Physicians India*. 1999;47(8):784-786.
9. Tariot PN, Sunderland T, Weingartner H, et al. Cognitive effects of L-deprenyl in Alzheimer's disease. *Psychopharmacology (Berl)*. 1987;91(4):489-495.
10. Sano M, Ernesto C, Thomas RG, et al. A controlled trial of selegiline, alpha-tocopherol, or both as treatment for Alzheimer's disease. The Alzheimer's Disease Cooperative Study. *N Engl J Med*. 1997;336:1216-1222.
11. Magni G, Meibach RC. Lazabemide for the long-term treatment of Alzheimer's disease. *Eur Neuropsychopharmacol*. 1999;9(Supplement 5):142. ISSN 0924-977X.
12. Nave S, Doody RS, Boada M. Sembragiline in Moderate Alzheimer's Disease: results of a Randomized, Double-Blind, Placebo-Controlled Phase II Trial (MAyflOwer RoAD). *J Alzheimers Dis*. 2017;58(4):1217-1228.
13. Schneider LS, Geffen Y, Rabinowitz J, et al. Low-dose ladostigil for mild cognitive impairment: a phase 2 placebo-controlled clinical trial. *Neurology*. 2019;93(15):e1474-e1484.
14. Kadir A, Andreasen N, Almkvist O. Effect of phenserine treatment on brain functional activity and amyloid in Alzheimer's disease. *Ann Neurol*. 2008;63(5):621-631.
15. Schmidt ME, Andrews RD, van der Ark P, et al. Dose-dependent effects of the CRF(1) receptor antagonist R317573 on regional brain activity in healthy male subjects. *Psychopharmacology (Berl)*. 2010;208(1):109-119.
16. Chen K, Langbaum JB, Fleisher AS, & Alzheimer's Disease Neuroimaging Initiative. Twelve-month metabolic declines in probable Alzheimer's disease and amnestic mild cognitive impairment assessed using an empirically pre-defined statistical region-of-interest: findings from the Alzheimer's Disease Neuroimaging Initiative. *Neuroimage*. 2010;51(2):654-64. quiz e423-6. PMID: 25199063; PMCID: PMC4332800.
17. Alexander GE, Chen K, Pietrini P, Rapoport SI, Reiman EM. Longitudinal PET evaluation of cerebral metabolic decline in dementia: a potential outcome measure in Alzheimer's Disease treatment studies. *Am J Psychiatry*. 2002;159(5):738-745.
18. Bouallègue F, Mariano-Goulart D, Payoux P, Alzheimer's Disease Neuroimaging Initiative (ADNI). Joint assessment of quantitative 18F-Florbetapir and 18F-FDG regional uptake using baseline data from the ADNI. *J Alzheimers Dis*. 2018;62(1):399-408.
19. Braak H, Alafuzoff I, Arzberger T, Kretzschmar H, Del Tredici K. Staging of Alzheimer disease-associated neurofibrillary pathology using paraffin sections and immunocytochemistry. *Acta Neuropathol*. 2006;112(4):389-404.

20. Maass A, Landau S, Baker SL, et al. Comparison of multiple tau-PET measures as biomarkers in aging and Alzheimer's disease. *Neuroimage*. 2017;157:448-463.
21. Pontecorvo MJ, Devous MD Sr, Navitsky M. 18F-AV-1451-A05 investigators. Relationships between flortaucipir PET tau binding and amyloid burden, clinical diagnosis, age and cognition. *Brain*. 2017;140(3):748-763.
22. Pontecorvo MJ, DeVous MD, Kennedy I. A multicentre longitudinal study of flortaucipir (18F) in normal ageing, mild cognitive impairment and Alzheimer's disease dementia. *Brain*. 2019;142(6).
23. Matthews DC, Lukic AS, Andrews RD. Dissociation of Down syndrome and Alzheimer's disease effects with imaging. *Alzheimers Dement (N Y)*. 2016;2(2):69-81.
24. Antonini A, Leenders KL, Vontobel P, et al. Complementary PET studies of striatal neuronal function in the differential diagnosis between multiple system atrophy and Parkinson's disease. *Brain*. 1997;120(Pt 12):2187-2195.
25. Kitaichi Y, Inoue T, Mitsui N. Selegiline remarkably improved stage 5 treatment-resistant major depressive disorder: a case report. *Neuropsychiatr Dis Treat*. 2013;9:1591-1594.
26. Strother S, Oder A, Spring R, Grady C. The NPAIRS Computational Statistics Framework for Data Analysis in Neuroimaging. In: Lechevallier Y, Saporta G, eds. *Proceedings of COMPSTAT'2010*. Physica-Verlag HD; 2010.
27. Southekal S, Devous MD Sr, Kennedy I, et al. Flortaucipir F 18 quantitation using parametric estimation of reference signal intensity. *J Nucl Med*. 2018;59(6):944-951.
28. Zubizarreta JR, Paredes RD, Rosenbaum PR. Matching for balance, pairing for heterogeneity in an observational study of the effectiveness of for-profit and not-for-profit high schools in Chile. *Ann Appl Stat*. 2014;8:204-231.
29. Egan MF, Kost J, Voss T. Randomized Trial of Verubecestat for Prodromal Alzheimer's Disease. *N Engl J Med*. 2019;380(15):1408-1420.
30. Klostermann EC, Braskie MN, Landau SM, O'Neil JP, Jagust WJ. Dopamine and fronto-striatal networks in cognitive aging. *Neurobiol Aging*. 2012;3(3):623.e15-623.e24.
31. Voruganti LN, Awad AG. Role of Dopamine in Pleasure, Reward and Subjective Responses to Drugs. In: Ritsner MS, Awad AG, eds. *Quality of Life Impairment in Schizophrenia, Mood and Anxiety Disorders*. Dordrecht: Springer; 2007.
32. Koch G, Motta C, Bonnì S, et al. Effect of rotigotine vs placebo on cognitive functions among patients with mild to moderate Alzheimer Disease: a randomized clinical trial. *JAMA Netw Open*. 2020;3(7):e2010372.
33. Kim EJ, Cho SS, Jeong Y, et al. Glucose metabolism in early onset versus late onset Alzheimer's disease: an SPM analysis of 120 patients. *Brain*. 2005;128(Pt 8):1790-1801.
34. Freedman NM, Mishani E, Krausz Y, et al. In vivo measurement of brain monoamine oxidase B occupancy by rasagiline, using (11)C-l-deprenyl and PET. *J Nucl Med*. 2005;46(10):1618-1624.
35. Ng KP, Therriault J, Kang MS, et al. Rasagiline, a monoamine oxidase B inhibitor, reduces in vivo [18F]THK5351 uptake in progressive supranuclear palsy. *Neuroimage Clin*. 2019;24:102091.
36. Tosun D, Landau S, Aisen PS, et al. Association between tau deposition and antecedent amyloid-β accumulation rates in normal and early symptomatic individuals. *Brain*. 2017;140(5):1499-1512.
37. Ossenkoppele R, Rabinovici GD, Smith R, et al. Discriminative Accuracy of [18F]flortaucipir Positron Emission Tomography for Alzheimer Disease vs Other Neurodegenerative Disorders. *JAMA*. 2018;320(11):1151-1162.
38. Sano M, Ernesto C, Thomas RG, et al. A controlled trial of selegiline, alpha-tocopherol, or both as treatment for Alzheimer's disease. The Alzheimer's Disease Cooperative Study. *N Engl J Med*. 1997;336(17):1216-1222. PMID: 9110909.
39. Rinne JO, Brooks DJ, Rossor MN, et al. 11C-PiB PET assessment of change in fibrillar amyloid-beta load in patients with Alzheimer's disease treated with bapineuzumab: a phase 2, double-blind, placebo-controlled, ascending-dose study. *Lancet Neurol*. 2010;9(4):363-372.

SUPPORTING INFORMATION

Additional supporting information may be found online in the Supporting Information section at the end of the article.

How to cite this article: Matthews DC, Ritter A, Thomas RG, et al. Rasagiline effects on glucose metabolism, cognition, and tau in Alzheimer's dementia. *Alzheimer's Dement*. 2021;7:e12106. https://doi.org/10.1002/trc2.12106

SUPPLEMENTAL MATERIAL FOR

Rasagiline effects on glucose metabolism, cognition, and tau in Alzheimer's dementia

Table of Contents

1. Tables referenced in main manuscript

Table S1. Clinical endpoint longitudinal results

Endpoint	24 week mean change (S.D.)		p-value
	Placebo	Rasagiline	
MMSE	1.14 (2.27)	0.65 (2.48)	n.s.
ADAS-cog	2.76 (4.30)	1.81 (4.43)	n.s.
ADL	3.23 (6.71)	3.75 (7.27)	n.s.
COWAT	1.09 (6.31)	-0.62 (5.55)	0.08
CGIC	n/a	n/a	n.s.
Digit Span	1.18 (1.92)	0.29 (3.08)	n.s.
NPI	2.00 (7.18)	0.20 (6.79)	n.s.
QoL-AD	1·95 (3·28)	-1·11 (3·77)	0.04

S.D. = standard deviation; Mod = moderate; n.s. = non-significant

Table S2. Adverse Events

Adverse Event	Placebo (n=25)		Rasagiline (n=25)	
	Number	Percent	Number	Percent
Abnormal Urinary Analysis	1	4%	2	8%
Agitation	2	8%	0	0%
Confusion	2	8%	2	8%
Delusions	3	12%	0	0%
Elevated blood pressure or cardiac related	2	8%	3	12%
Elevated thyroid stimulating hormone	1	4%	2	8%
Fall	1	4%	2	8%
Insomnia	2	8%	0	0%
Rash / skin lesion	1	4%	2	8%

Number of subjects (%) with adverse events who received 1 or more doses of study drug (occurring in 5% or more in either treatment group).

2. Figures referenced in main manuscript

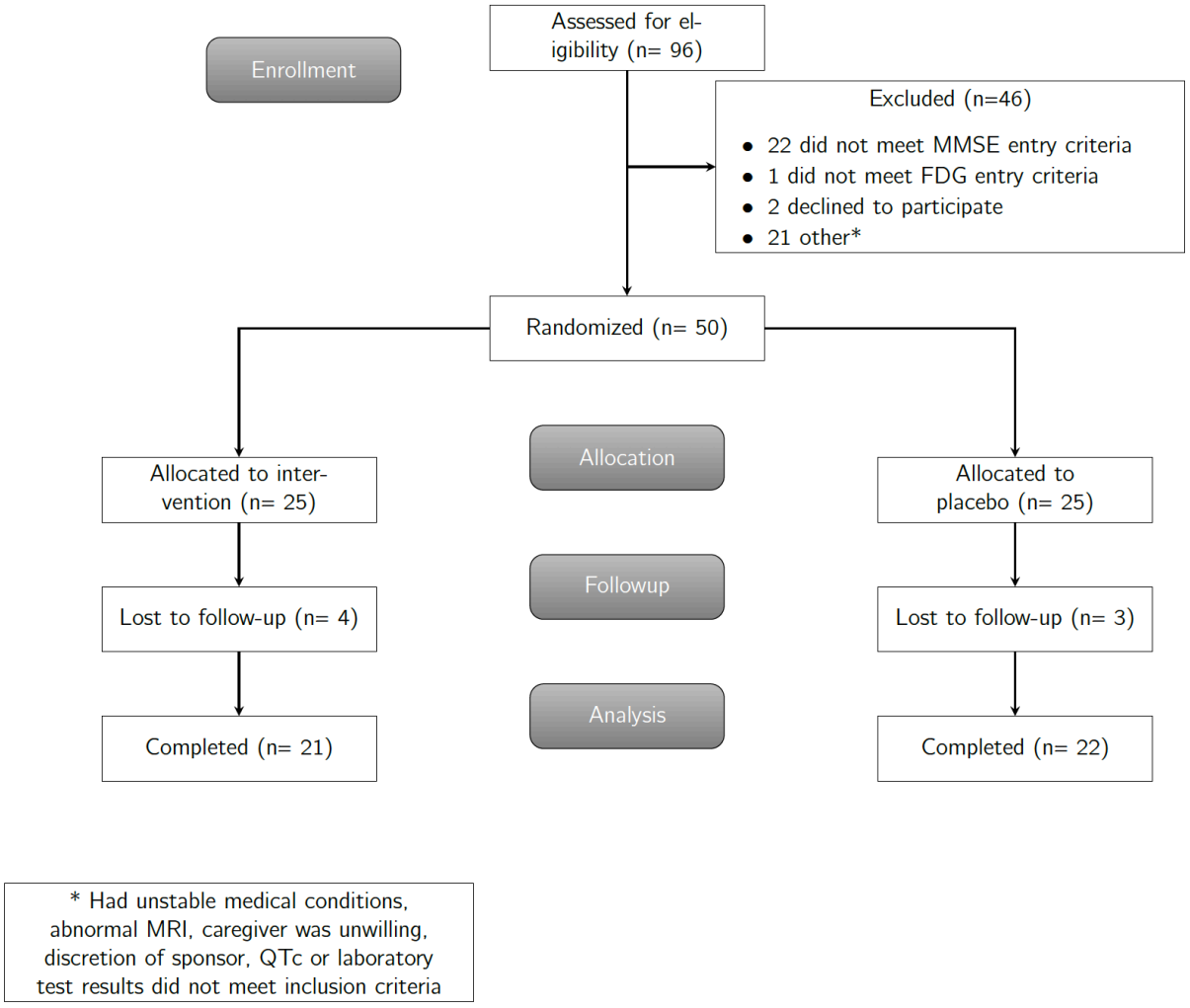

Figure S1. Consort diagram: flow of patients through the trial

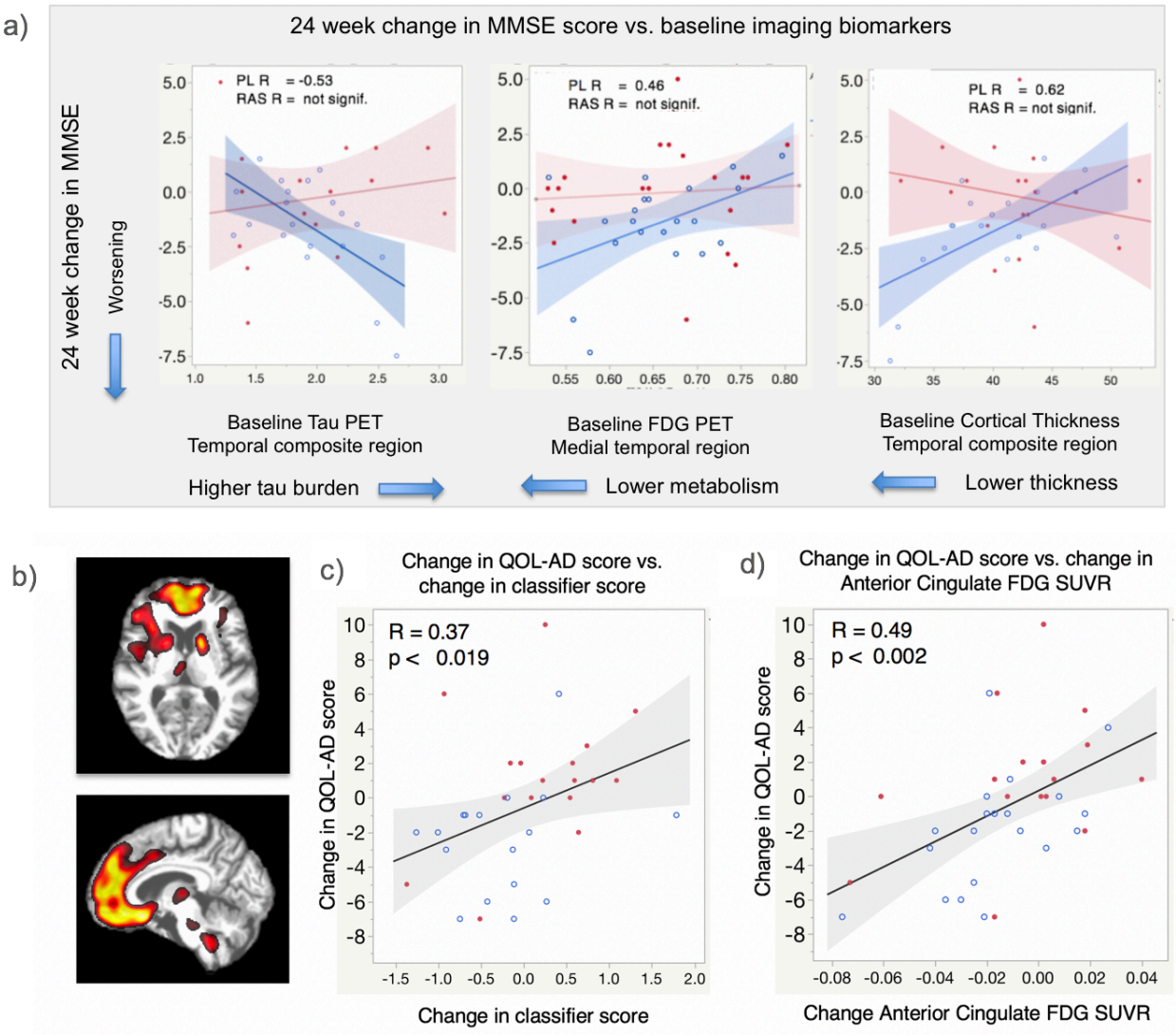

Figure S2. a) Twenty-four week change in MMSE scores vs. baseline temporal tau SUVRs, FDG PET SUVRs, and cortical thickness. Blue = placebo, Red = rasagiline. b) Classifier pattern of glucose metabolism increases (orange) associated with greater QoL-AD scores. c) Relationship between change in classifier score for pattern in (b) and change in QoL-AD score. Placebo = open blue circles, rasagiline-treated = solid red circles. d) Relationship between Anterior Cingulate FDG SUVR (pre-specified region of interest that is part of the classifier pattern) and change in QoL-AD score.

3. Imaging Methods

Image acquisition protocols were consistent with those used in the Alzheimer's Disease Neuroimaging Initiative (ADNI)(www.adni-info.org) as described below.

3.1. MRI

Volumetric MR images of 3T field strength were acquired at three imaging sites using a 3D magnetization prepared rapid gradient echo (MPRAGE) T1 weighted scan with field of view (FOV) = 256 × 256 × 160; voxel size = 1 × 1 × 1.2 mm^3; TR = 2300 ms, TE = 2.98 ms; TI = 900 ms and flip angle = 9° or similar MPRAGE parameters.

MRI scans were visually inspected for anatomical inclusion, subject motion, and other artifacts. MRI scans were processed using Freesurfer version 6.0[13,14] to produce regional segmentation masks with measurements of volume and cortical thickness. This processing included N3 correction for nonuniformities. MRI scans were also spatially transformed to a template in Montreal Neurological Institute (MNI) space using statistical parametric mapping (SPM12)[1]. Freesurfer segmentation results were visually inspected, and volume values were corrected for total intracranial volume (ICV) as calculated using the gray, white, and cerebrospinal (CSF) segments determined by SPM12.

3.2. FDG PET

Image Acquisition

FDG PET scans were acquired using 5 mCi FDG with an uptake time of 20 minutes during which participants were at rest but awake in a dimly lit room with eyes and ears open. Sleep medications such as zolpidem were disallowed on the evening prior to FDG PET scans. Emission scans were acquired over a 30-minute period comprised of six five-minute frames following a transmission scan used for attenuation correction. Participants were monitored to confirm conformance to the at-rest protocol during uptake and were monitored for motion during image acquisition. At-rest requirements included refraining from movement, conversation, or sleep during FDG uptake. Reconstruction was performed using Ordered subset expectation maximization (OSEM).[2]

Image Processing

FDG PET scans were visually inspected for participant motion and other artifacts. Multi-frame images were motion corrected and averaged into static images that were smoothed using a Gaussian filter. The 24-week PET scans were co-registered to baseline PET scans, which had been co-registered to their respective MRI scans. Volumetric masks generated by Freesurfer 6.0 were visually inspected and used to measure the signal intensities from the co-registered PET scans, as individual or composite regions. In addition, the spatial transforms determined for the MRI scans were applied to the PET scans to enable voxel-based comparisons using images in template space.

For FDG PET SUVR measurement, the reference region was based upon spatial clusters found to be metabolically preserved during the progression of AD based upon our prior development of a voxel-based multivariate classifier ("AD Progression Classifier"[3]). These reference clusters included

paracentral gyrus and subregions of pons and cerebellar vermis, similar to preserved clusters identified by Chen et al[4]. However, the striatum was omitted due to reported metabolic change associated with rasagiline in this region. Longitudinal results were compared to those obtained using whole brain (minus ventricles) and subcortical white matter reference regions to verify that effects were not specific to the primary reference region.

Endpoints

FDG Standardized Uptake Value ratios (SUVRs) were measured in the following prespecified regions of interest associated with progressive hypometabolism in AD: medial temporal, lateral temporal, posterior cingulate-precuneus, inferior parietal, and middle frontal. The anterior cingulate and striatum were also prespecified given prior findings of correlation between dopamine and glucose metabolism in those regions[5] and reported selegiline effects on FDG in striatum associated with clinical benefit[6].

Images were also evaluated using both apriori and data driven machine learning classifiers. In brief, these classifiers were developed using the NPAIRS framework[7,8], which performs feature reduction using Principal Component analysis followed by Canonical Variate Analysis, coupled with many iterations of split half resampling. In each iteration, the half data sets are treated as training and test data sets. The models derived from each half are compared to one another using correlation, producing a metric of reproducibility. Each half is also used as the test half for the other half, and the classification accuracy for the test subjects produces a quantitative prediction measure. These parameters are then used to determine consensus patterns of relative hypo- and hyper- (or preserved) metabolism that differentiate classes while minimizing risk of overfitting. The degree to which each individual participant scan expresses each pattern is captured by a Canonical Variate score, which can then be analyzed using descriptive statistics.

Two previously developed (apriori) FDG PET classifiers were applied at baseline to determine whether participants exhibited metabolic patterns associated with AD as compared to those of individuals with several other dementias:

1. The Dementia Differentiation Classifier identifies the probability of association with a combination of patterns that characterize the following different types of dementia (or lack of disease): Normal amyloid negative, MCI amyloid positive, AD amyloid positive, Severe AD amyloid positive, frontal (behavioral) variant Frontotemporal Dementia (FTD), semantic variant FTD, and Lewy Body Disease.

2. The AD Progression Classifier quantifies the degree to which a scan expresses a pattern of hypometabolism and preservation relative to whole brain that reflects the progression from cognitively normal amyloid negative status to amyloid positive MCI and AD dementia, as described in Matthews et. al.[3]

The data driven classifier that was included as one of the FDG primary endpoints (Figure 2 in the main manuscript) was derived by defining classes based upon study arm, stratified by younger and older age groups, and using the difference scans between 24 weeks and baseline as the inputs.

Participant Inclusion/Exclusion

Participants were excluded from longitudinal FDG PET analysis if major behavioral confounds occurred during FDG uptake, if motion was so severe that it could not be adequately corrected, or if other protocol deviation or image artifact was identified that would prevent proper signal measurement. Of the 42 participants who had baseline and 24-week FDG PET scans available, two participants from the placebo group and one participant from the rasagiline group were excluded due to major behavioral confounds during the FDG uptake period and/or severe motion during image acquisition. Longitudinal analyses were conducted using this set of 39 participants.

3.3. Flortaucipir PET

Image acquisition

Tau PET scans were acquired using 10 mCi of the radiotracer AV-1451, in four 5 minute frames from 80 to 100 minutes post tracer injection, following a transmission scan. All PET scans were acquired using a Siemens mCT PET scanner, at two sites. Reconstruction was performed using Ordered subset expectation maximization (OSEM)[2].

Image processing and measurement

Flortaucipir PET scans were visually inspected, motion corrected, averaged into static images, and smoothed using a Gaussian filter. The 24-week scans were co-registered to the baseline scan, which was coregistered to the baseline MRI. Regions of interest as defined by Freesurfer 6.0 were then measured in native space. In addition, the flortaucipir scans were spatially transformed to template space by applying the transform determined for the MRI to which they were coregistered.

Baseline flortaucipir SUVRs were first evaluated using a cerebellar cortex reference region thresholded to exclude spillover from adjacent tissue and high intensity clusters that can create signal artifact[9]. For longitudinal evaluation, the following reference regions were compared: cerebellar cortex, and a calculated white matter reference mean that mathematically reduces the effects of spillover from adjacent high signal tissue based on a Gaussian 2-mixture model (PERSI)[10]. Use of white matter was motivated by previous findings demonstrating that reference regions incorporating subcortical white matter have shown lower variance and greater effect sizes than cerebellar cortex in longitudinal measurement of tau[11,12] and amyloid[13–16]. SUVRs derived from these reference regions were compared using the following criteria: (a) cross-sectional range for baseline values and (b) variability (signal to noise) for longitudinal measurements. Longitudinal SUVRs were evaluated using the reference region with least longitudinal variability for the study population overall.

The cerebellar cortex provided the best reference region to examine the range of cross-sectional tau burden. All reference regions produced SUVrs compatible with visually apparent tau burden. However, those referenced to white matter showed less differentiation between tau burden levels due to gray signal spillover into the white matter reference in participants with high tau burden. The PERSI approach mitigated the impact of spillover, reducing the white matter reference values by up to 26% (and thus increasing target region SUVRs). However, values for participants with extensive tau were still somewhat reduced as compared to SUVRs based on cerebellum, beyond that accounted for by the generally higher tracer signal expected in white matter. For longitudinal measurement, white matter reference regions (with or without the PERSI adjustment) were associated with less

directional variability then cerebellar cortex, and the PERSI reference was used for longitudinal SUVR evaluation.

Flortaucipir SUVRs were measured in total cortical gray tissue excluding cerebellum, a composite temporal region (CTR) consisting of entorhinal cortex, amygdala, parahippocampal gyrus, inferior temporal, and middle temporal regions[16], the regions measured for FDG PET, and additional cortical and subcortical regions defined on MRI using Freesurfer 6.0. These included composite regions based on the six stages identified by Braak[17,18]; and the regions measured for FDG PET. An additional adaptive region approach was evaluated in which the region of interest was comprised of suprathreshold voxels from the baseline scan "Or'd" (the union) with those in the 24 week scan. Effects of rasagiline upon flortaucipir binding were also explored by examining longitudinal change in putamen, accumbens, thalamus, and brainstem.

Partial volume correction effects were examined at baseline in some subjects using the Müller-Gärtner method[19] as implemented using PMOD software but did not impact overall results. A 24 week MRI was not acquired and partial volume correction was not applied for longitudinal analysis over this relatively short timeframe of 24 weeks.

Participant inclusion/exclusion

Participants were excluded from group analyses for tau PET if the start time for emission scan acquisition differed between baseline and 24-week visits by more than 5 minutes, due to published time-dependent increases in flortaucipir signal that occur during the acquisition time window[20]. Adjustment for acquisition start time differences in tau PET scans, as in Pontecorvo et al[21], was deferred for future exploration. Four participants were excluded from the longitudinal analysis due to acquisition timing.

4. Longitudinal Tau PET (Secondary Outcome Measure)

The 24-week effects of rasagiline on tau burden were evaluated in this study. Since rasagiline is a potent selective MAO-B inhibitor, longitudinal measurement also posed a sensitive within-subject challenge to detect potential off-target binding of flortaucipir to MAO-B.

As noted in the main manuscript text, using a PERSI white matter reference region, longitudinal flortaucipir SUVRs exhibited stability or increases in cortical regions including precuneus, inferior parietal, lateral occipital, and total cortex (not including cerebellar cortex). In subjects with very low / no tau (flortaucipir binding), some decreases were observed but no overall difference between study arms was observed. Slight mean decreases were observed in the rasagiline arm but not in the placebo arm in anterior cingulate (not significant when comparing the two study arms) and insula (trend level of $p<0{\cdot}08$).

Decreases were noted in the rasagiline arm in several subcortical regions while mean placebo arm values were unchanged. These regions and p-values associated with the comparison of placebo change to treatment arm change included accumbens ($p<0{\cdot}001$), putamen ($p<0{\cdot}003$), pallidum ($p<0{\cdot}02$), thalamus ($p<0{\cdot}05$), and brainstem ($p<0{\cdot}03$). Subcortical decreases in the rasagiline arm were also found when using cerebellar cortex as a reference region (Figure S3).

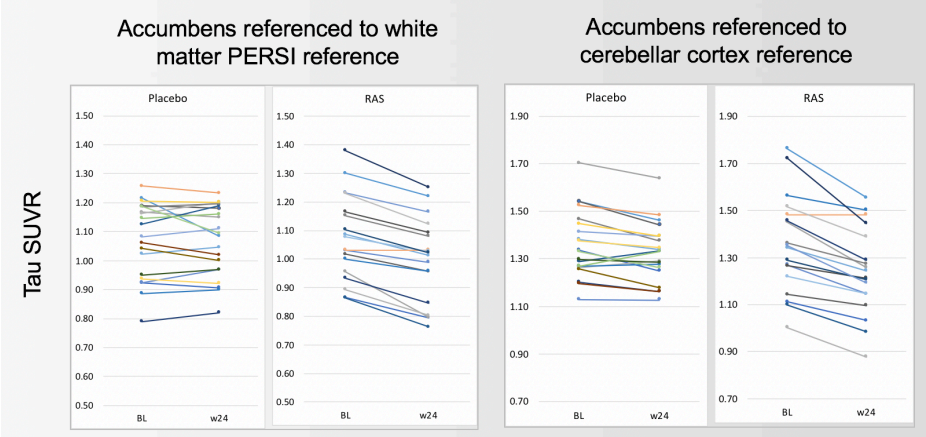

Figure S3. Longitudinal change in accumbens. Individual participant SUVRs are shown at baseline and 24 weeks, referenced to the PERSI white matter region and to cerebellar cortex for comparison. Subcortical decreases are observed in the rasagiline arm but not the placebo arm for both reference regions.

The following potential contributors to the subcortical decreases in rasagiline arm were considered as discussed below: 1) removal of tau; 2) changes in SUVR associated with changes in local blood flow rate; 3) tracer interaction with MAO-B; 4) tracer interaction with a different off-target entity.

1) *Removal of tau*. Although tau has been identified in the putamen[22] of some AD patients, increases observed in flortaucipir binding in putamen, pallidum, and thalamus appear to be related to age rather than to amyloid status or AD progression[23]. In the accumbens, where the most uniform reductions in flortaucipir signal occurred with rasagiline, only limited tau aggregation has been observed in AD[24]. Studies have suggested that flortaucipir signal in subcortical regions may be associated with off-target binding[25,26]. If flortaucipir reductions in the rasagiline arm are due to tau removal, reductions in cortical regions might be expected but were not observed. These considerations suggest that the subcortical reductions in flortaucipir signal may be associated with factors other than removal of tau.

2) *Impact of blood flow changes on SUVR*. Increases in regional blood flow can decrease measured SUVR.[27] However, flortaucipir decreases in the rasagiline arm in caudate, brainstem, and accumbens do not correlate with local increases in FDG, which is often but not always closely coupled with blood flow. Further, the decreases observed in the rasagiline arm are relatively uniform in contrast to the more variable changes observed in FDG or that might be expected in a treatment response. If blood flow is responsible for the SUVR decreases, the lack of correlation could be because blood flow recruitment tends to be an "on/off" event. The role of blood flow could be determined using full dynamic scans and kinetic modeling but is not suggested by the present data.

3) *Flortaucipir binding to MAO-B*. Although flortaucipir has not been found to bind strongly to MAO-B in cross-sectional comparisons[28,29], it binds weakly in vitro to MAO-B[30,31]. The decreases observed in the rasagiline arm are in regions established to be associated with higher MAO-B concentrations and with which rasagiline is known to interact as demonstrated by Freedman.[32] However, the reductions observed in the present study were far less than those

shown by Freedman, as well as the signal depletion of [18F]THK5351, a tracer with strong MAO-B affinity, following rasagiline treatment.[33] Within the striatum, the accumbens has been reported in preclinical evaluation to most strongly express MAO-B[34], and it was in this region that rasagiline related decreases were most uniform. However, the lack of decreases in other cortical regions where MAO-B is known to reside suggest that any MAO-B affinity is weak and superseded by that to tau.

The potential inconsistency between the findings of Smith (lack of apparent cross-sectional affinity) and those of Drake and others (weak in vitro binding) was resolved by examining differences between the placebo and rasagiline arms cross sectionally and with respect to 24-week change. The pallidum was used to approximate the globus pallidus (dorsal pallidum) used by Smith. Figure S4 illustrates the finding that for SUVRs based on either the PERSI or cerebellar reference region, within-subject decreases are not significant relative to intra-subject, cross sectional SUVR variability. Therefore, while the groups do not differ cross-sectionally, their longitudinal change differs significantly. This was also tested and confirmed in the accumbens region. Therefore, the findings by Smith et al, findings by Drake et al, and MAO-B as a possible source of rasagiline related flortaucipir decreases are not inconsistent with one another.

A comparison of these modest yet significant reductions in subcortical flortaucipir signal to the complete depletion of MAO-B by rasagiline demonstrated by Freedman[32] also suggests that MAO-B binding by flortaucipir is weak.

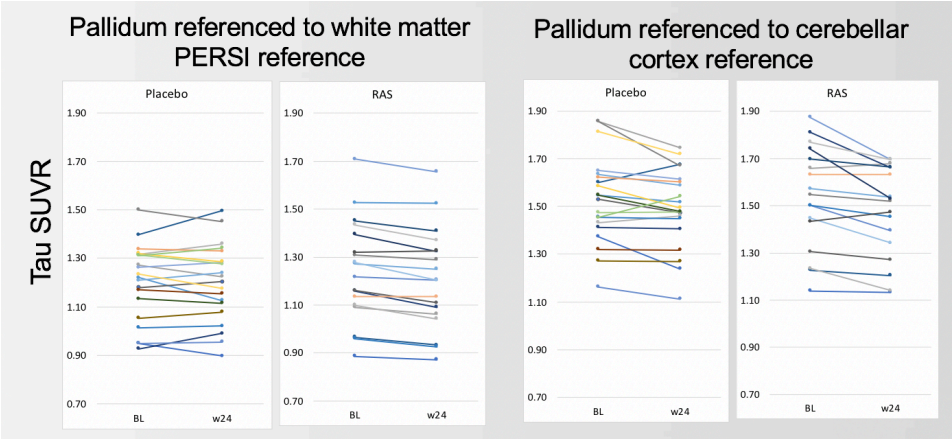

Figure S4. Baseline and 24-week SUVRs in pallidum referenced to white matter PERSI reference and cerebellar cortex reference for placebo and rasagiline arms. The decrease in the rasagiline arm does not create a significant difference in cross sectional comparisons across study arms.

4) *Other off-target binding.* It is less likely that another off-target entity has the same binding distribution as MAO-B and would be affected by a selective MAO-B inhibitor, unless this entity is highly similar to MAO-B.

The subcortical decreases observed do not impact baseline patient characterization or comparisons across imaging and clinical measures. They do suggest caution when interpreting changes in flortaucipir SUVR in subcortical regions in the rasagiline study.

5. Supplemental Clinical Endpoint Results (Secondary Outcome Measures)

5.1. Mild and Moderate Subgroups

Table S3. Moderate Subgroup Baseline Characteristics.

	Placebo (N=10)	Rasagiline (N=4)	All (N=14)	p-value
Age (S.D.), range (years)	74·3 (6·8) (61–84)	66·3 (5·0) (62–73)	72·0 (7·2) (61–84)	0·5
Sex (Female/Male)	0·5/0·5	0·75/0·25	0·57/0·43	0·6
Education	14·6 (2·0)	15·3 (1·5)	14·8 (1·8)	0·8
MMSE	14·6 (2·5)	15·3 (3·4)	14·8 (2·7)	0·06
ADAScog-11	36·4 (9·9)	29·3 (1·3)	34·4 (8·9)	0·06
ADL	51·3 (7·1)	55·8 (1·3)	52·6 (6·3)	0·2
COWAT	15·8 (9·6)	13.3 (7·4)	15·1 (8·8)	0·13
Digit Span	11·9 (3·3)	10·8 (2·6)	11·6 (3·1)	0·13
NPI	8·0 (10·4)	12·0 (9·7)	9·1 (10·0)	0·8
QoL-AD	38·2 (5·0)	30·0 (3·4)	35·7 (5·9)	0·02
Site (1/2/3)	0·6/0·2/0·2	0·5/0·25/0·25	0·57/0·21/0·21	1·0
APOE4 (carrier/non)	0·7/0·3	0·75/0·25	0·71/0·29	0·5

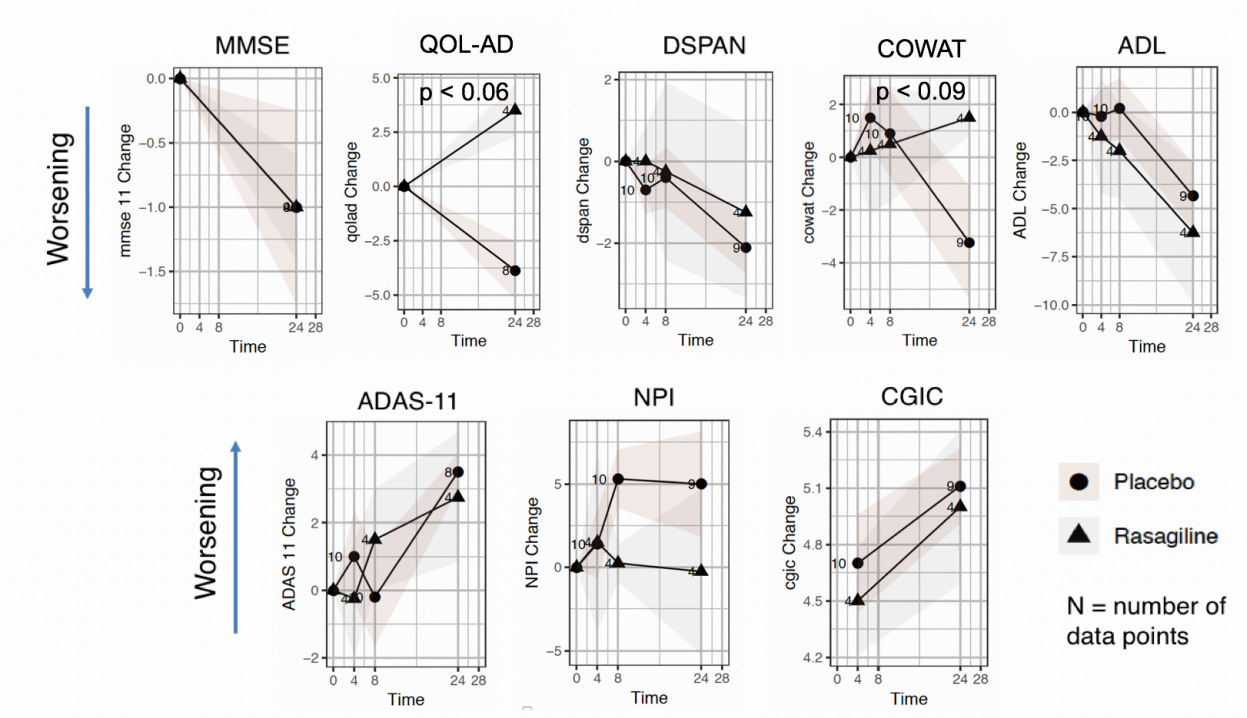

Figure S5. Longitudinal clinical endpoints in the moderate subgroup.

Table S4. Mild Subgroup Baseline Characteristics.

	Placebo (N=15)	Rasagiline (N=21)	All (N=36)	p-value
Age (S.D.), range (years)	72·9 (7·5) (57–84)	76·3 (6·6) (63–90)	74·9 (7·1) (57–90)	0·5
Sex (Female/Male)	0·4/0·6	0·52/0·48	0·47/0·53	0·6
Education	13·8 (2·5)	14·1 (3·0)	14·0 (2·8)	0·8
MMSE	22·0 (3·0)	22·4 (2·2)	22·2 (2·5)	0·06
ADAScog-11	22·3 (6·5)	22·1 (5·9)	22·2 (6·0)	0·06
ADL	62·8 (11·0)	63·1 (8·7)	63·0 (9·6)	0·2
COWAT	24·7 (14·3)	29·3 (11·8)	27·4 (12·9)	0·13
Digit Span	11·7 (3·3)	13·5 (2·6)	12·8 (3·0)	0·13
NPI	8·5 (8·3)	6·8 (7·1)	7·5 (7·6)	0·8
QoL-AD	40·4 (5·4)	38·2 (4·5)	39·2 (5·0)	0·02
Site (1/2/3)	0·4/0·47/0·13	0·52/0·38/0·1	0·47/0·42/0·11	1·0
APOE4 (carrier/non)	0·87/0·13	0·65/0·35	0·73/0·27	0·5

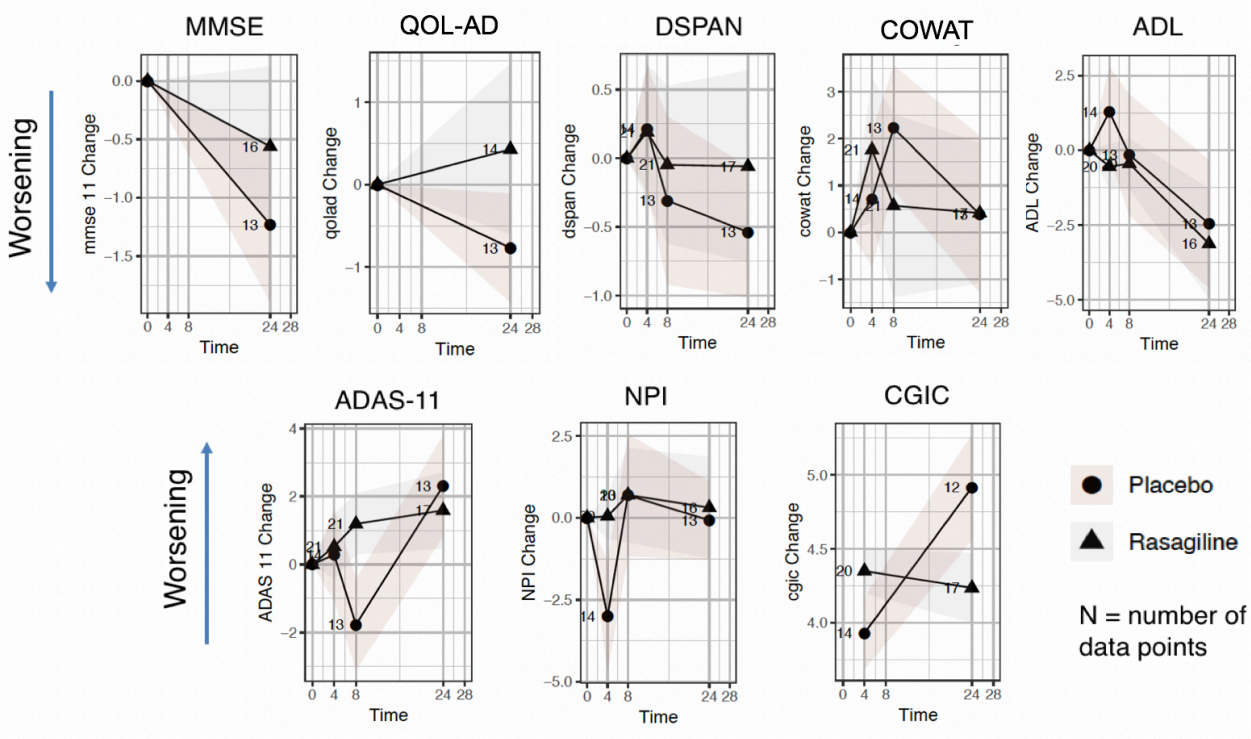

Figure S4. Longitudinal clinical endpoints in the mild subgroup.

5.2. Female and Male Subgroups

Table S5. Female Subgroup Baseline Characteristics.

	Placebo (N=11)	Rasagiline (N=14)	All (N=25)	p-value
Age (S.D.), range (years)	73·6 (7·4) (61–84)	74·8 (7·2) (63–85)	74·3 (7·2) (61–85)	0·5
Sex (Female/Male)	1·0/0·0	1·0/0·0	1·0/0·0	n/a
Education	13·1 (2·0)	13·6 (2·7)	13·4 (2·4)	0·8
MMSE	18·5 (4·6)	24·3 (6·4)	25·9 (8·8)	0·06
ADAScog-11	27·9 (11·1)	22·1 (5·9)	22·2 (6·0)	0·06
ADL	58·7 (10·3)	59·7 (10·0)	59·3 (9·9)	0·2
COWAT	19·6 (10·4)	27·3 (14·6)	23·9 (13·3)	0·13
Digit Span	11·6 (2·5)	13·4 (3·0)	12·6 (2·9)	0·13
NPI	8·1 (9·9)	6·6 (4·3)	7·3 (7·2)	0·8
QoL-AD	39·3 (5·6)	36·1 (6·4)	37·7 (6·1)	0·02
Site (1/2/3)	0·45/0·27/0·27	0·64/0·21/0·14	0·56/0·24/0·20	1·0
APOE4 (carrier/non)	0·64/0·36	0·77/0·23	0·70/0·30	0·5

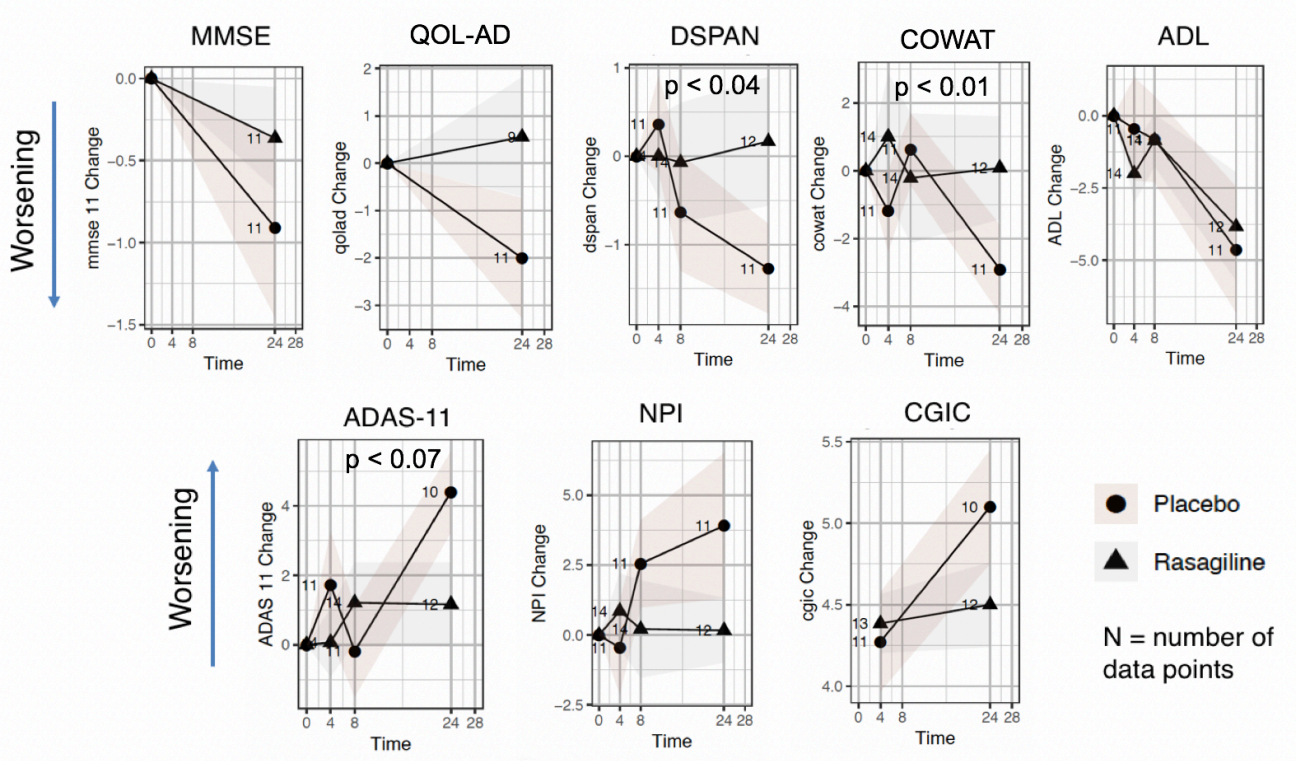

Figure S5. Longitudinal clinical endpoints in the female subgroup.

Table S6. Male Subgroup Baseline Characteristics.

	Placebo (N=14)	Rasagiline (N=11)	All (N=25)	p-value
Age (S.D.), range (years)	73·3 (7·2) (57–84)	74·6 (7·9) (62–90)	73·9 (7·4) (57–90)	0·5
Sex (Female/Male)	0·0/1·0	0·0/1·0	0·0/1·0	n/a
Education	14·9 (2·2)	15·1 (2·9)	15·0 (2·5)	0·8
MMSE	19·5 (4·7)	22·6 (2·3)	20·9 (4·1)	0·06
ADAScog-11	28·0 (10·5)	21·8 (5·5)	25·3 (9·1)	0·06
ADL	57·8 (12·1)	64·9 (4·4)	60·8 (10·1)	0·2
COWAT	22·4 (15·3)	26·0 (10·1)	24·0 (13·1)	0·13
Digit Span	11·9 (3·8)	12·6 (2·5)	12·2 (3·2)	0·13
NPI	8·4 (8·5)	9·0 (10·9)	8·7 (9·4)	0·8
QoL-AD	39·9 (5·1)	37·4 (4·3)	38·7 (4·8)	0·02
Site (1/2/3)	0·5/0·43/0·07	0·36/0·55/0·09	0·44/0·48/0·08	1·0
APOE4 (carrier/non)	0·93/0·07	0·54/0·45	0·72/0·28	0·5

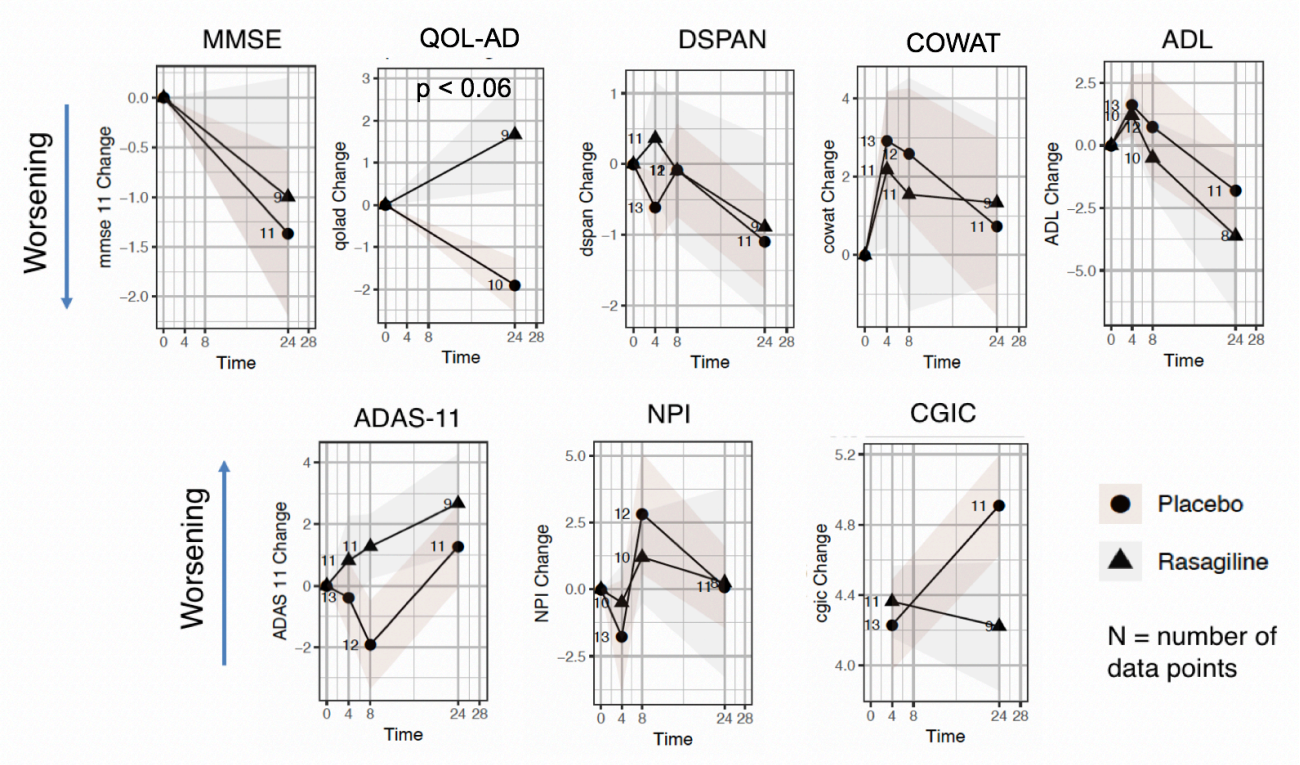

Figure S6. Longitudinal clinical endpoints in the male subgroup.

5.3. Younger and Older Subgroups

Table S7. Younger Subgroup Baseline Characteristics

	Placebo (N=8)	Rasagiline (N=9)	All (N=17)	p-value
Age (S.D.), range (years)	65·0 (4·8) (57–71)	67·0 (3·5) (62–71)	66·1 (4·2) (57–71)	0·5
Sex (Female/Male)	0·38/0·62	0·44/0·56	0·41/0·59	0·6
Education	15·3 (2·2)	14·7 (1·7)	14·9 (1·9)	0·8
MMSE	19·3 (6·1)	19·6 (4·6)	19·4 (5·2)	0·06
ADAScog-11	29·4 (14·8)	22·9 (6·3)	25·9 (11·2)	0·06
ADL	59·3 (8·3)	62·4 (6·6)	60·8 (7·4)	0·2
COWAT	24·9 (19·0)	23·9 (2·7)	24·0 (13·1)	0·13
Digit Span	11·9 (3·8)	12·6 (2·5)	12·5 (3·3)	0·13
NPI	9·6 (10·0)	4·4 (8·8)	6·9 (9·5)	0·8
QoL-AD	40·7 (4·0)	35·5 (5·8)	37·9 (5·6)	0·02
Site (1/2/3)	0·5/0·5/0·0	0·44/0·33/0·22	0·47/0·41/0·12	1·0
APOE4 (carrier/non)	0·75/0·25	0·78/0·22	0·76/0·24	0·5

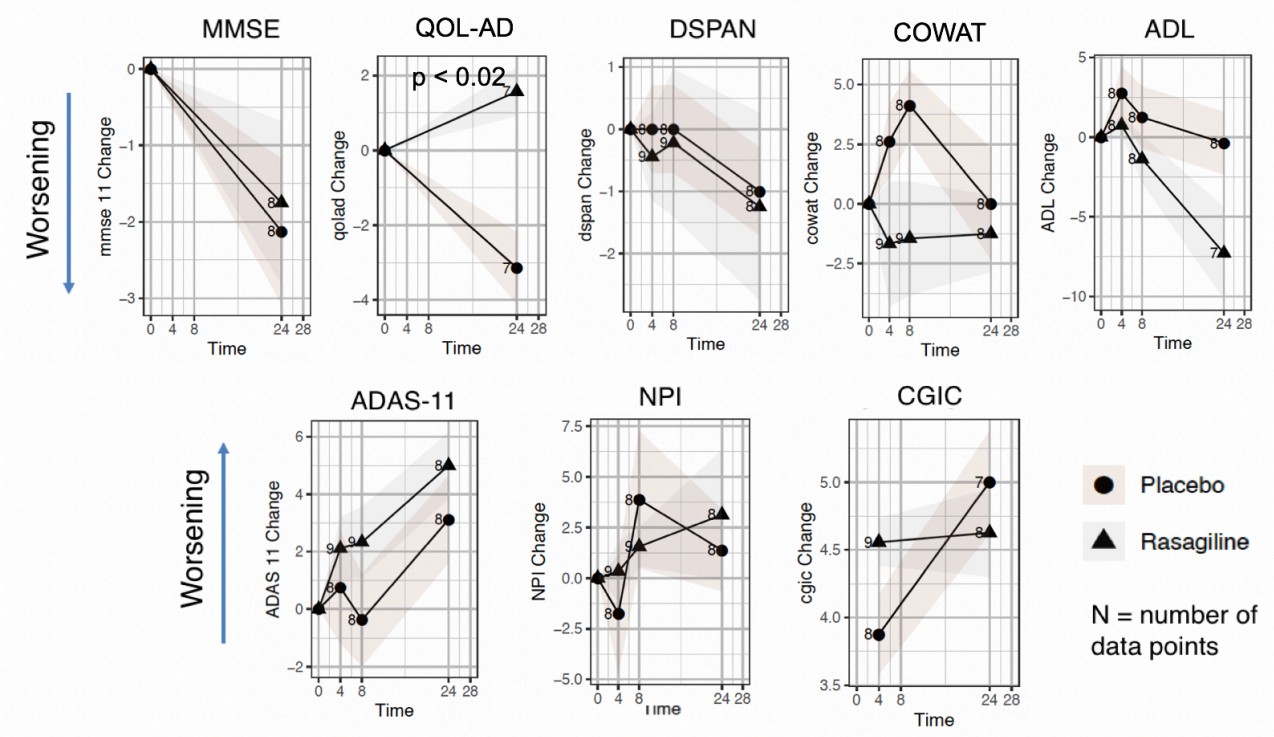

Figure S7. Longitudinal clinical endpoint in the younger subgroup.

Table S8. Older Subgroup Baseline Characteristics

	Placebo (N=17)	Rasagiline (N=16)	All (N=33)	p-value
Age (S.D.), range (years)	77·4 (3·7) (72–84)	79·1 (4·9) (72–90)	78·2 (4·3) (72–90)	0·5
Sex (Female/Male)	0·47/0·53	0·62/0·38	0·55/0·45	0·6
Education	13·6 (2·2)	14·1 (3·3)	13·8 (2·8)	0·8
MMSE	18·9 (3·9)	22·2 (2·5)	20·5 (3·6)	0·06
ADAScog-11	27·3 (8·3)	23·4 (6·0)	25·4 (7·5)	0·06
ADL	57·7 (12·4)	61·6 (9·4)	59·6 (11·1)	0·2
COWAT	19·4 (9·6)	28·3 (11·2)	23·7 (11·2)	0·13
Digit Span	11·7 (2·9)	13·2 (2·9)	12·4 (3·0)	0·13
NPI	7·7 (8·7)	9·5 (6·4)	8·5 (7·6)	0·8
QoL-AD	39·1 (5·7)	37·4 (5·2)	38·4 (5·5)	0·02
Site (1/2/3)	0·47/0·29/0·24	0·56/0·38/0·06	0·52/0·33/0·15	1·0
APOE4 (carrier/non)	0·83/0·17	0·60/0·40	0·72/0·28	0·5

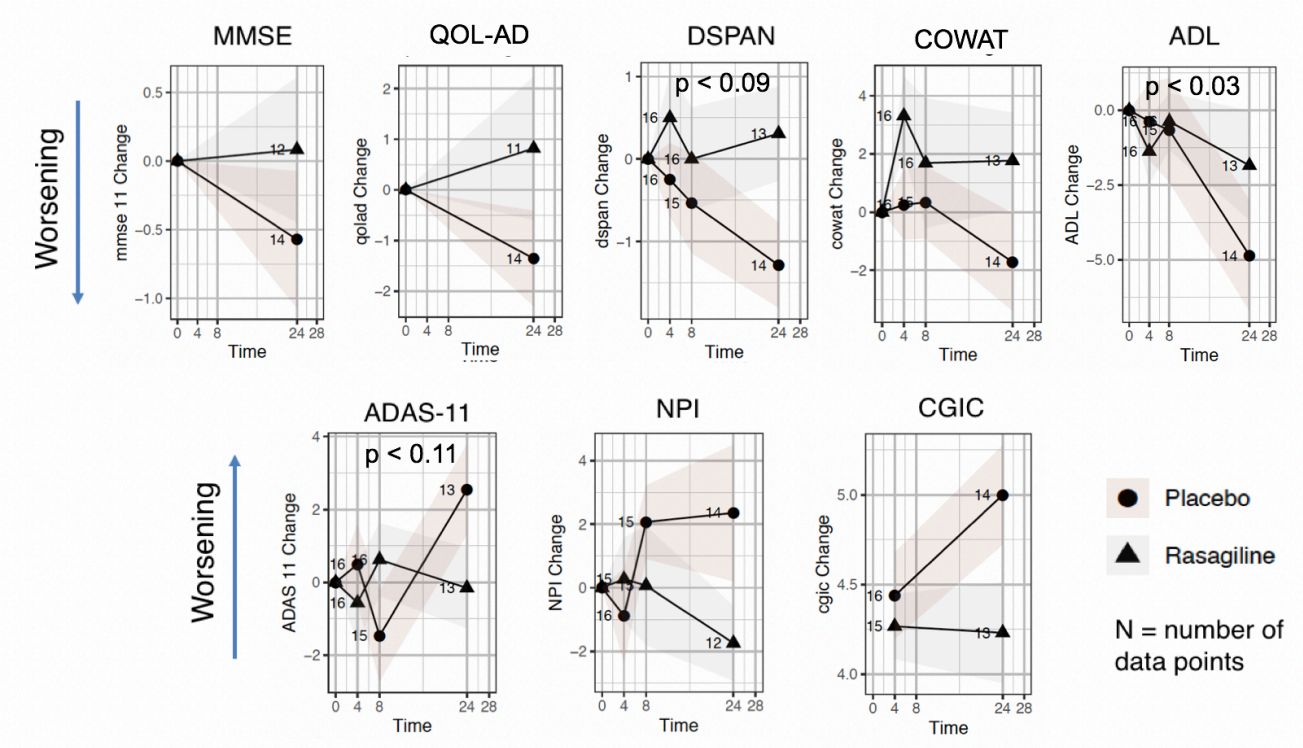

Figure S8. Longitudinal clinical endpoints in the older subgroup.

6. Supplemental References

[1] Ashburner J. A Fast Diffeomorphic Image Registration Algorithm. NeuroImage, 38(1):95-113, 2007.

[2] Hudson, HM, Larkin, RS. Accelerated image reconstruction using ordered subsets of projection data. IEEE Trans. Medical Imaging, 1994: 13 (4), 601–609.

[3] Matthews DC, Lukic AS, Andrews RD, et. al. Dissociation of Down syndrome and Alzheimer's disease effects with imaging. Alzheimers Dement (N Y). 2016 Jun;2(2):69-81.

[4] Chen K, Roontiva A, Thiyyagura P, Lee W, Liu X, Ayutyanont N, Protas H, Luo JL, Bauer R, Reschke C, Bandy D, Koeppe RA, Fleisher AS, Caselli RJ, Landau S, Jagust WJ, Weiner MW, Reiman EM; Alzheimer's Disease Neuroimaging Initiative. Improved power for characterizing longitudinal amyloid-β PET changes and evaluating amyloid-modifying treatments with a cerebral white matter reference region. J Nucl Med. 2015 Apr;56(4):560-6.

[5] Antonini A, Leenders KL, Vontobel P, Maguire RP, Missimer J, Psylla M, Günther I. Complementary PET studies of striatal neuronal function in the differential diagnosis between multiple system atrophy and Parkinson's disease. Brain. 1997 Dec;120 (Pt 12):2187-95.

[6] Kitaichi Y, Inoue T, Mitsui N, et. al. Selegiline remarkably improved stage 5 treatment-resistant major depressive disorder: a case report. Neuropsychiatr Dis Treat. 2013;9:1591-4. doi: 10.2147/NDT.S49261.

[7] Strother SC, Older A, Spring R, Grady C. The NPAIRS Computational Statistics Framework for Data Analysis in Neuroimaging. Proceedings of COMPSTAT'2010 pp 111-120

[8] Strother SC, Anderson J, Hansen LK, Kjems U, Kustra R, Sidtis J, Frutiger S, Muley S, LaConte S, Rottenberg D. The quantitative evaluation of functional neuroimaging experiments: the NPAIRS data analysis framework. Neuroimage. 2002 Apr;15(4):747-71.

[9] Baker SL, Maass A, Jagust WJ. Considerations and code for partial volume correcting [18F]-AV-1451 tau PET data. Data Brief. 2017 Oct 16;15:648-657. Data Brief. 2017 Oct 16;15:648-657.

[10] Southekal S, Devous MD Sr, Kennedy I, Navitsky M, Lu M, Joshi AD, Pontecorvo MJ, Mintun MA. Flortaucipir F 18 Quantitation Using Parametric Estimation of Reference Signal Intensity. J Nucl Med. 2018 Jun;59(6):944-951. doi: 10.2967/jnumed.117.200006.

[11] Cho H, Choi JY, Lee HS, Lee JH, Ryu YH, Lee MS, Jack CR Jr, Lyoo CH. Progressive tau accumulation in Alzheimer's disease: two-year follow-up study. J Nucl Med. 2019 Mar 29.

[12] Fleisher AS, Joshi AD, Sundell KL, Chen YF, Kollack-Walker S, Lu M, Chen S, Devous MD Sr, Seibyl J, Marek K, Siemers ER, Mintun MA. Use of white matter reference regions for detection of change in florbetapir positron emission tomography from completed phase 3 solanezumab trials. Alzheimers Dement. 2017 Oct;13(10):1117-1124.

[13] Chen K, Roontiva A, Thiyyagura P, Lee W, Liu X, Ayutyanont N, Protas H, Luo JL, Bauer R, Reschke C, Bandy D, Koeppe RA, Fleisher AS, Caselli RJ, Landau S, Jagust WJ, Weiner MW, Reiman EM; Alzheimer's Disease Neuroimaging Initiative. Improved power for characterizing longitudinal amyloid-β PET changes and evaluating amyloid-modifying treatments with a cerebral white matter reference region. J Nucl Med. 2015 Apr;56(4):560-6. doi: 10.2967/jnumed.114.149732.

[14] Landau SM, Fero A, Baker SL, Koeppe R, Mintun M, Chen K, Reiman EM, Jagust WJ. Measurement of longitudinal β-amyloid change with 18F-florbetapir PET and standardized uptake value ratios. J Nucl Med. 2015 Apr;56(4):567-74.

[15] Schwarz CG, Senjem ML, Gunter JL, Tosakulwong N, Weigand SD, Kemp BJ, Spychalla AJ, Vemuri P, Petersen RC, Lowe VJ, Jack CR Jr. Optimizing PiB-PET SUVR change-over-time measurement by a large-scale analysis of longitudinal reliability, plausibility, separability, and correlation with MMSE. Neuroimage. 2017 Jan 1;144(Pt A):113-127.

[16] Jack CR Jr, Wiste HJ, Schwarz CG, Lowe VJ, Senjem ML, Vemuri P, Weigand SD, Therneau TM, Knopman DS, Gunter JL, Jones DT, Graff-Radford J, Kantarci K, Roberts RO, Mielke MM, Machulda MM, Petersen RC. Longitudinal tau PET in ageing and Alzheimer's disease. Brain. 2018 May 1;141(5):1517-1528.

[17] Braak H, Alafuzoff I, Arzberger T, Kretzschmar H, Del Tredici K. Staging of Alzheimer disease-associated neurofibrillary pathology using paraffin sections and immunocytochemistry. Acta Neuropathol. 2006 Oct;112(4):389-404.

[18] Schöll M, Lockhart SN, Schonhaut DR, O'Neil JP, Janabi M, Ossenkoppele R, Baker SL, Vogel JW, Faria J, Schwimmer HD, Rabinovici GD, Jagust WJ. PET Imaging of Tau Deposition in the Aging Human Brain. Neuron. 2016 Mar 2;89(5):971-982.

[19] Müller-Gärtner HW, Links JM, Prince JL, Bryan RN, McVeigh E, Leal JP, Davatzikos C, Frost JJ. Measurement of radiotracer concentration in brain gray matter using positron emission tomography: MRI-based correction for partial volume effects. J Cereb Blood Flow Metab. 1992 Jul;12(4):571-83.

[20] Shcherbinin S, Schwarz A, Joshi A, Navitsky M, Flitter M, Shankle WR, Devous MD, Mintun MA. Kinetics of the Tau PET Tracer 18F-AV-1451 (T807) in Subjects

[21] Pontecorvo MJ, DeVous MD, Kennedy I, et. al. A multicentre longitudinal study of flortaucipir (18F) in normal ageing, mild cognitive impairment and Alzheimer's disease dementia. Brain April 2019. Brain, Volume 142, Issue 6, June 2019, Pages 1723–1735.

[22] Hamasaki H, Honda H, Suzuki SO, Shijo M, Ohara T, Hatabe Y, Okamoto T, Ninomiya T, Iwaki T. Tauopathy in basal ganglia involvement is exacerbated in a subset of patients with Alzheimer's disease: The Hisayama study. Alzheimers Dement (Amst). 2019 Jun 6;11:415-423. doi: 10.1016/j.dadm.2019.04.008.

[23] Lowe VJ, Wiste HJ, Senjem ML, Weigand SD, Therneau TM, Boeve BF, Josephs KA, Fang P, Pandey MK, Murray ME, Kantarci K, Jones DT, Vemuri P, Graff-Radford J, Schwarz CG, Machulda MM, Mielke MM, Roberts RO, Knopman DS, Petersen RC, Jack CR Jr. Widespread brain tau and its association with ageing, Braak stage and Alzheimer's dementia. Brain. 2018 Jan 1;141(1):271-287.

[24] Kawakami I, Hasegawa M, Arai T, Ikeda K, Oshima K, Niizato K, Aoki N, Omi K, Higashi S, Hosokawa M, Hirayasu Y, Akiyama H. Tau accumulation in the nucleus accumbens in tangle-predominant dementia. Acta Neuropathol Commun. 2014 Apr 8;2:40. doi: 10.1186/2051-5960-2-40.

[25] Marquié M, Normandin MD, Vanderburg CR, et. al. Validating novel tau positron emission tomography tracer [F-18]-AV-1451 (T807) on postmortem brain tissue. Ann Neurol. 2015 Nov;78(5):787-800. doi: 10.1002/ana.24517. Epub 2015 Sep 25. PMID: 26344059; PMCID: PMC4900162.

[26] Shcherbinin S, Schwarz AJ, Joshi A, Navitsky M, Flitter M, Shankle WR, Devous MD Sr, Mintun MA. Kinetics of the Tau PET Tracer 18F-AV-1451 (T807) in Subjects with Normal Cognitive Function, Mild Cognitive Impairment, and Alzheimer Disease. J Nucl Med. 2016 Oct;57(10):1535-1542.

[27] van Berckel BN, Ossenkoppele R, Tolboom N, Yaqub M, Foster-Dingley JC, Windhorst AD, Scheltens P, Lammertsma AA, Boellaard R. Longitudinal amyloid imaging using 11C-PiB: methodologic considerations. J Nucl Med. 2013 Sep;54(9):1570-6. doi: 10.2967/jnumed.112.113654.

[28] Smith R, Schöll M, Londos E, Ohlsson T, Hansson O. 18F-AV-1451 in Parkinson's Disease with and without dementia and in Dementia with Lewy Bodies. Sci Rep. 2018 Mar 16;8(1):4717. doi: 10.1038/s41598-018-23041-x.

[29] Hansen AK1, Brooks DJ2,3,4, Borghammer P. MAO-B Inhibitors Do Not Block In Vivo Flortaucipir([18F]-AV-1451) Binding. Mol Imaging Biol. 2018 Jun;20(3):356-360. doi: 10.1007/s11307-017-1143-1.

[30] Drake LR, Pham JM, Desmond TJ, Mossine AV, Lee SJ, Kilbourn MR, Koeppe RA, Brooks AF, Scott PJH. Identification of AV-1451 as a Weak, Nonselective Inhibitor of Monoamine Oxidase. ACS Chem Neurosci. 2019 Aug 5. doi: 10.1021/acschemneuro.9b00326.

[31] Vermeiren C, Motte P, Viot D, Mairet-Coello G, Courade JP, Citron M, Mercier J, Hannestad J, Gillard M. The tau positron-emission tomography tracer AV-1451 binds with similar affinities to tau fibrils and monoamine oxidases. Mov Disord. 2018 Feb;33(2):273-281. doi: 10.1002/mds.27271. Epub 2017 Dec 26.

[32] Freedman NM, Mishani E, Krausz Y, Weininger J, Lester H, Blaugrund E, Ehrlich D, Chisin R. In vivo measurement of brain monoamine oxidase B occupancy by rasagiline, using (11)C-l-deprenyl and PET. J Nucl Med. 2005 Oct;46(10):1618-24.

[33] Ng KP, Therriault J, Kang MS, et al. Rasagiline, a monoamine oxidase B inhibitor, reduces in vivo [18F]THK5351 uptake in progressive supranuclear palsy. Neuroimage Clin. 2019;24:102091. doi:10.1016/j.nicl.2019.102091

[34] Ikemoto K, Kitahama K, Maeda T, Tokunaga Y, Valatx JL, De Maeyer E, Seif I. Electron-microscopic study of MAOB-containing structures in the nucleus accumbens shell: using MAOA-deficient transgenic mice. Brain Res. 1997 Oct 10;771(1):163-6.